Journal of Pharmaceutical Analysis 13 (2023) 1135–1152

Contents lists available at ScienceDirect

Journal of Pharmaceutical Analysis

journal homepage: www.elsevier.com/locate/jpa

Original article

Monoclonal antibody targeting mu-opioid receptor attenuates morphine tolerance via enhancing morphine-induced receptor endocytosis

Jia-Jia Zhang [a, 1], Chang-Geng Song [b, 1], Miao Wang [a], Gai-Qin Zhang [a], Bin Wang [a], Xi Chen [c], Peng Lin [a], Yu-Meng Zhu [a], Zhi-Chuan Sun [d], Ya-Zhou Wang [e], Jian-Li Jiang [a], Ling Li [a], Xiang-Min Yang [a, **], Zhi-Nan Chen [a, *]

[a] National Translational Science Center for Molecular Medicine & Department of Cell Biology, Fourth Military Medical University, Xi'an, 710032, China
[b] Department of Neurology, Xijing Hospital, Fourth Military Medical University, Xi'an, 710032, China
[c] Key Laboratory of Synthetic and Natural Functional Molecule of the Ministry of Education, College of Chemistry and Materials Science, Northwest University, Xi'an, 710032, China
[d] Department of Neurosurgery, Xi'an Daxing Hospital, Xi'an, 710032, China
[e] Department of Neurobiology and Institute of Neurosciences, Collaborative Innovation Center for Brain Science, School of Basic Medicine, Fourth Military Medical University, Xi'an, 710032, China

ARTICLE INFO

Article history:
Received 6 March 2023
Received in revised form
28 May 2023
Accepted 20 June 2023
Available online 20 June 2023

Keywords:
Morphine tolerance
Mu-opioid receptor
Endocytosis
Monoclonal antibody
Physical dependence

ABSTRACT

Morphine is a frequently used analgesic that activates the mu-opioid receptor (MOR), which has prominent side effects of tolerance. Although the inefficiency of morphine in inducing the endocytosis of MOR underlies the development of morphine tolerance, currently, there is no effective therapy to treat morphine tolerance. In the current study, we aimed to develop a monoclonal antibody (mAb) precisely targeting MOR and to determine its therapeutic efficacy on morphine tolerance and the underlying molecular mechanisms. We successfully prepared a mAb targeting MOR, named 3A5C7, by hybridoma technique using a strategy of deoxyribonucleic acid immunization combined with cell immunization, and identified it as an immunoglobulin G mAb with high specificity and affinity for MOR and binding ability to antigens with spatial conformation. Treatment of two cell lines, HEK293T and SH-SY5Y, with 3A5C7 enhanced morphine-induced MOR endocytosis via a G protein-coupled receptor kinase 2 (GRK2)/β-arrestin2-dependent mechanism, as demonstrated by immunofluorescence staining, flow cytometry, Western blotting, coimmunoprecipitation, and small interfering ribonucleic acid (siRNA)-based knockdown. This mAb also allowed MOR recycling from cytoplasm to plasma membrane and attenuated morphine-induced phosphorylation of MOR. We established an in vitro morphine tolerance model using differentiated SH-SY5Y cells induced by retinoic acid. Western blot, enzyme-linked immunosorbent assays, and siRNA-based knockdown revealed that 3A5C7 mAb diminished hyperactivation of adenylate cyclase, the in vitro biomarker of morphine tolerance, via the GRK2/β-arrestin2 pathway. Furthermore, in vivo hotplate test demonstrated that chronic intrathecal administration of 3A5C7 significantly alleviated morphine tolerance in mice, and withdrawal jumping test revealed that both chronic and acute 3A5C7 intrathecal administration attenuated morphine dependence. Finally, intrathecal electroporation of silencing short hairpin RNA illustrated that the in vivo anti-tolerance and anti-dependence efficacy of 3A5C7 was mediated by enhanced morphine-induced MOR endocytosis via GRK2/β-arrestin2 pathway. Collectively, our study provided a therapeutic mAb, 3A5C7, targeting MOR to treat morphine tolerance, mediated by enhancing morphine-induced MOR endocytosis. The mAb 3A5C7 demonstrates promising translational value to treat clinical morphine tolerance.

Peer review under responsibility of Xi'an Jiaotong University.
* Corresponding author.
** Corresponding author.
E-mail addresses: znchen@fmmu.edu.cn (Z.-N. Chen), yxiangmind@163.com (X.-M. Yang).
[1] Both authors contributed equally to this work.

https://doi.org/10.1016/j.jpha.2023.06.008

1. Introduction

Chronic pain is a major health issue affecting approximately one-third of population in the Western countries, which reduces quality of life and costs an annual economic burden of approximately 600 billion USD [1]. Opioids are the most frequently used analgesics against severe pain, especially in controlling chronic pain [2]. However, repeated or long-term use of morphine and other opioids can lead to tolerance [3]. Morphine tolerance is characterized by a reduction in analgesic efficacy following prolonged drug administration [4], resulting in dose escalation to reach the same analgesic effects, longer hospital stay, poorer compliance, and higher risk of complications and addictions [5–7]. Current strategies to treat morphine tolerance include dose increasing, opioid switching, or providing extra-opioid analgesia [4]. However, none of these strategies targets the molecular mechanism underlying the pathogenesis of tolerance, nor can they prevent the development of tolerance from the beginning of morphine therapy.

Endocytosis is a conserved cellular process existing among eukaryotes, which transports a wide range of extracellular cargos and receptors from the plasma membrane into intracellular compartments, where they can be recycled back to the plasma membrane, targeted to lysosomes for degradation, or targeted to other destinations, such as the Golgi apparatus or nucleus, for specific functions [8,9]. Endocytosis, which is achieved via distinct endocytic pathways, controls the composition of the plasma membrane and the interactions between cells and their environments [10]. Thus, endocytosis is crucial in the regulation of cellular functions such as signal transduction, cell cycle and proliferation, synaptic neurotransmission, apoptosis, and nutrient intake [11]. Endocytosis participates in pathological conditions. It is not only involved in the entrance of pathogens or toxins into cells [12,13] but also plays important roles in the development of multiple diseases, including atherosclerosis, tumor metastasis, diabetes, and neurodegenerative diseases [14–17].

The key molecular mechanism of morphine tolerance is its inefficiency in inducing the endocytosis of mu-opioid receptor (MOR), the receptor of morphine and a member of the inhibitory G protein-coupled receptor (GPCR) family [18]. After binding to opioids, MOR is desensitized by G protein-coupled receptor kinases (GRKs), and MOR phosphorylated by GRKs recruits β-arrestin2, which further leads to receptor endocytosis, recycling to the membrane, and resensitization [19]. Hence, endocytosis is an important mechanism to ensure that desensitized MOR is rapidly internalized and recycled back to the cell surface in an active form, maintaining MOR signaling and reducing MOR desensitization and the development of tolerance. Moreover, chronic morphine exposure triggered prolonged signaling through MOR that contributed to secondary adaptations involved in tolerance, whereas endocytosis of MOR terminated prolonged signaling and limited secondary adaptations and tolerance [19,20]. However, compared with other MOR agonists, such as [D-Ala^2, *N*-MePhe^4, Gly-ol]-enkephalin (DAMGO), fentanyl, and endorphin, morphine has a poor ability to induce the endocytosis of MOR [21,22]. Therefore, desensitized MOR is poorly internalized and resensitized, contributing to both acute and chronic tolerance to morphine. Facilitating the endocytosis of MOR during morphine treatment provides a promising strategy to counteract morphine tolerance. Nevertheless, currently there is no available therapy to achieve this goal effectively.

Antibodies targeting GPCRs represent promising options to modulate the functions of GPCRs and to treat GPCR-related disorders [23]. Compared with small-molecule drugs that are usually agonists or antagonists, antibodies exhibit superior specificity to the diverse conformations of GPCRs, longer serum half-life, and fewer adverse effects [24]. However, due to the high conformational variability, small exposed area of extracellular epitopes, and difficulty in preparing active forms of GPCR antigens suitable for antibody isolation [24,25], preparing therapeutic antibodies targeting GPCRs remains a challenge for drug development and translation. In this study, we successfully developed a monoclonal antibody (mAb) targeting MOR with high affinity and specificity, which could promote the endocytosis of MOR and thus attenuate morphine tolerance. We investigated the molecular mechanisms underlying the endocytosis-promoting effects of this MOR-targeting mAb and revealed that the mAb targeting MOR had promising potential to treat morphine tolerance as a GPCR antibody therapeutic.

2. Materials and methods

2.1. Reagents and antibody preparation

Retinoic acid (RA), DAMGO, naloxone, and monensin were purchased from Sigma-Aldrich (St. Louis, MO, USA). A lactic dehydrogenase (LDH) assay kit was purchased from Nanjing Jiancheng Bioengineering Institute (Nanjing, China). Morphine hydrochloride was purchased from Takeda Pharmaceuticals (Tokyo, Japan). The mouse monoclonal anti-Na^+/K^+-ATPase α1 subunit antibody (sc-21712) was purchased from Santa Cruz Biotechnology (Dallas, TX, USA). The goat monoclonal anti-Rab5 antibody (orb153348) was purchased from Biorbyt (Cambridge, UK). The mouse monoclonal anti-glyceraldehyde 3-phosphate dehydrogenase (GAPDH) antibody (60004-1-Ig), rabbit polyclonal anti-lysosome associated membrane protein-1 (LAMP-1) antibody (21997-1-AP), rabbit polyclonal anti-GRK2 antibody (13990-1-AP), and rabbit polyclonal anti-β-arrestin2 antibody (10171-1-AP) were purchased from Proteintech (Chicago, IL, USA). The rabbit polyclonal anti-phospho-MOR Serine 375 (p-MOR) antibody (#3,451), rabbit polyclonal anti-protein kinase A (PKA) antibody (#4,782), and rabbit polyclonal anti-tubulin antibody (#2,146) were purchased from Cell Signaling Technology (Danvers, MA, USA). Alexa 488-conjugated donkey anti-mouse immunoglobulin G (IgG), Alexa 555-conjugated donkey anti-rabbit IgG, neomycin (G418), and mouse IgG were purchased from Thermo Fisher Scientific Inc. (Waltham, MA, USA).

The development and preparation of the mAb targeting MOR, named 3A5C7, was based on a previous study [26] and is shown in Figs. S1 and S2. The general procedure for developing 3A5C7 is illustrated in Figs. S1A and B. First, human *OPRM* (NCBI: NM_000914), the gene encoding MOR, was amplified from a human complementary DNA (cDNA) library (Fig. S1C), and the sequence was optimized as shown in Fig. S1D to increase expression efficiency. Second, recombinant vectors overexpressing MOR were constructed by cloning the optimized *OPRM* sequence into the pCI-neo vector between the *EcoR I* and *Not I* restriction sites to obtain the recombinant pCI-neo-MOR vector (Fig. S1E). DNA sequencing (Fig. S1F) and nucleic acid electrophoresis (Fig. S2A) confirmed that the *OPRM* sequence had been correctly inserted into the vector and that the recombinant pCI-neo-MOR vector was successfully constructed. Third, cells stably overexpressing MOR were constructed. HEK293T and Renca cells were transfected with the recombinant pCI-neo-MOR vector using lipofectamine 2000 (Invitrogen, Carlsbad, CA, USA) and the transfected cells were selected with G418 after 48 h for approximately 30 days. The expression of MOR in transfected cells was determined by Western blot and the constructed cells stably overexpressing MOR were named HEK293T-MOR or Renca-MOR (Figs. S2B and C). Fourth, mice were immunized with the recombinant pCI-neo-MOR vector and Renca-MOR cells to generate antibodies targeting ectopically expressed MOR with a strategy of DNA immunization combined with cell boost immunization. Four female Balb/c mice aged 5 weeks were injected subcutaneously with the pCI-neo-MOR

plasmid (1 μg/μL, 100 μL) three times with 14-day intervals between each injection. Fourteen days after the last plasmid injection, Renca-MOR cells (1×10^7 in 200 μL) were repeatedly frozen and thawed three times to remove their tumorigenic ability and were intraperitoneally injected into the mice (200 μL/mouse). The serum antibody titers of the four mice were detected on the 14th day after the third plasmid injection (before the cell injection) and the 7th day after the cell injection using enzyme-linked immunosorbent assay (ELISA) (Figs. S2D and E). Fifth, B cells were extracted from the mouse with the highest serum antibody titer and were fused with hybridoma cells. The hybridoma technique and limited dilution method were used to produce monoclones, and six monoclonal strains were obtained through multiple fusion and screening (Fig. S2F). Next, we investigated whether these six monoclonal strains could produce antibodies (secreted into the supernatant) targeting MOR and the degree of binding between the antibodies and MOR using Western blot (Fig. S2F) and flow cytometry (Figs. S2G–I), and the monoclonal strain with clonal number 3A5C7B12D11B9G5 was identified to produce the mAb targeting MOR with optimal binding ability. The mAb secreted by the 3A5C7B12D11B9G5 strain was enriched with ascites amplification, purified, and named as 3A5C7.

The characteristics of mAb 3A5C7, including the immunoglobulin subtype, specificity, affinity, and binding ability to antigen with spatial conformation were then identified with Coomassie blue staining, Western blot, ELISA, immunofluorescence, flow cytometry, and isothermal titration calorimetry (ITC). The ITC experiment, specifically, was performed to confirm the binding between mAb 3A5C7 and MOR antigen on a MicroCal iTC200 titration calorimeter (GE HealthCare, Northampton, MA, USA). Briefly, 1×10^7 HEK293T and HEK293T-MOR cells were collected, resuspended in 500 μL of phosphate buffered saline (PBS) and added to the sample pool. One milligram of 3A5C7 mAb was suspended in 50 μL of PBS and added to the microinjector as titration solution. Under the control of the titration calorimeter, 2 μL of antibody solution was dripped into the sample pool every 2 min at 4 °C for 50 min, and the alterations in the reaction heat of antigen-antibody binding were recorded. The appearance of reaction heat peaks indicated that the antigen and antibody had a binding effect.

2.2. Cell cultures

HEK293T cells were cultured in the medium Roswell Park Memorial Institute (RPMI) 1640 (Life Technologies, Carlsbad, CA, USA) supplemented with 10% (*V*/*V*) fetal bovine serum (FBS; Gibco, Carlsbad, CA, USA) at 37 °C with 5% carbon dioxide. HEK293T-MOR were cultured in RPMI 1640 supplemented with 10% (*V*/*V*) FBS and 800 μg/mL G418. SH-SY5Y cells were cultured in Dulbecco's modified eagle medium (DMEM) (Life Technologies) supplemented with 10% (*V*/*V*) FBS and 10 μM RA.

2.3. Animals

Male C57BL/6 (B6) mice (20–25 g) were housed at 2–5 per cage and maintained under a 12 h light/dark cycle at 23 °C with food and water available ad libitum. All animal experiments were approved by the Committee on the Ethics of Animal Experiments of Fourth Military Medical University and conducted in accordance with the institutional standards of animal care (Approval No.: IACUC-20230018).

2.4. Small interfering ribonucleic acid (siRNA) transfection

The siRNAs directed against the messenger RNA (mRNA) of *GRK2* (5′-AAGAAGUACGAGAAGCUGGAGtt-3′), *ARRB2* (5′-AAGGACCGCA AAGUGUUUGUGtt-3'; the gene encoding human β-arrestin2), and the universal negative control (5′-AAUUCUCCGAACGUGUCACGUtt-3′) were synthesized by Sangon Biotech (Shanghai, China). Cells were transfected with the siRNA using lipofectamine 2,000 reagent (Invitrogen) according to the manufacturer's instructions. After 48 h, total RNA and whole cell lysates were extracted to determine the efficiency of siRNA interference by real-time polymerase chain reaction (PCR) and Western blot.

2.5. Real-time PCR

The expression of GRK2 and β-arrestin2 in cells was examined using real-time PCR. Total RNA from the cell lines was extracted using an RNA isolation kit (OMEGA, Norcross, GA, USA) and reverse transcribed into cDNA with a PrimeScript RT reagent kit (TAKARA Bio, Shiga, Japan). The cDNA was used as the template for real-time PCR analysis on an ABI 7200 analyzer (Applied Biosystems, Foster, CA, USA) with SYBR Green I (TAKARA Bio) as the fluorescent probe. Relative expression levels of the genes were normalized to the expression of housekeeping gene *GAPDH*. All primers were synthesized by BGI Genomics (Beijing, China) as follows: *GRK2*, forward primer 5′-GGACAGTGATCAGGAGCTCTA-3′ and reverse primer 5′-AAGGACTGCATCATGCATGGC-3'; *ARRB2*, forward primer 5′-GTCGAGCCCTAACTGCAAG-3′ and reverse primer 5′-ACAAACACTTTGCGGTCCTTC-3'; *GAPDH*, forward primer 5′-AGAAGGCTGGGGCTCATTTG-3′ and reverse primer 5′-AGGGGCCATCCACAGTCTTC-3'. Real-time quantitative PCR was performed with a miniOpticon system (Bio-Rad, Hercules, CA, USA). The conditions for amplification were one cycle of 94 °C for 4 min and 45 cycles of 94 °C for 20 s, 58 °C for 20 s, and 72 °C for 20 s. All PCR reactions were performed in triplicate. The cycle threshold (CT) value was determined as the point at which the fluorescence exceeded a preset limit by the instrument's software (Opticon monitor, version 3.1). The relative mRNA expression of the target gene was calculated by the ΔCT method, and the amount of target gene relative to GAPDH mRNA was expressed as $2^{-\Delta\Delta CT}$.

2.6. Western blot

Radioimmunoprecipitation assay buffer (Sigma-Aldrich) supplemented with protease inhibitor cocktail (Roche, Burgess Hill, UK) and phosphorylation inhibitor cocktail (Roche) was used to extract total protein from cells and tissues. The protein concentration of each sample was determined by a bicinchoninic acid (BCA) kit (Thermo Fisher Scientific Inc.). Thirty micrograms of the extracted protein was loaded and separated by 10% sodium dodecyl sulfate (SDS)-polyacrylamide gel electrophoresis (PAGE) and then electrophoretically transferred to a polyvinylidene fluoride membrane (Hybond; Amersham Biosciences, Little Chalfont, UK). Membranes were blocked with 5% nonfat milk powder in tris buffered saline plus tween for 1 h at room temperature. These membranes were incubated at 4 °C overnight with the anti-MOR antibody (ab137460; Abcam, Boston, MA, USA), anti-p-MOR antibody, anti-GRK2 antibody, anti-β-arrestin2 antibody, and anti-PKA antibody. The protein antibody immune complexes were detected with horseradish peroxidase-conjugated secondary antibodies (Invitrogen) and enhanced chemiluminescence reagents (Pierce Biotechnology, Rockford, IL, USA). GAPDH or tubulin was used as an internal control to calculate the ratio of optical density, and values were compared with those of controls.

2.7. Flow cytometry analysis

Internalization and recycling of MOR were assessed using fluorescence-activated cell sorting analysis as described

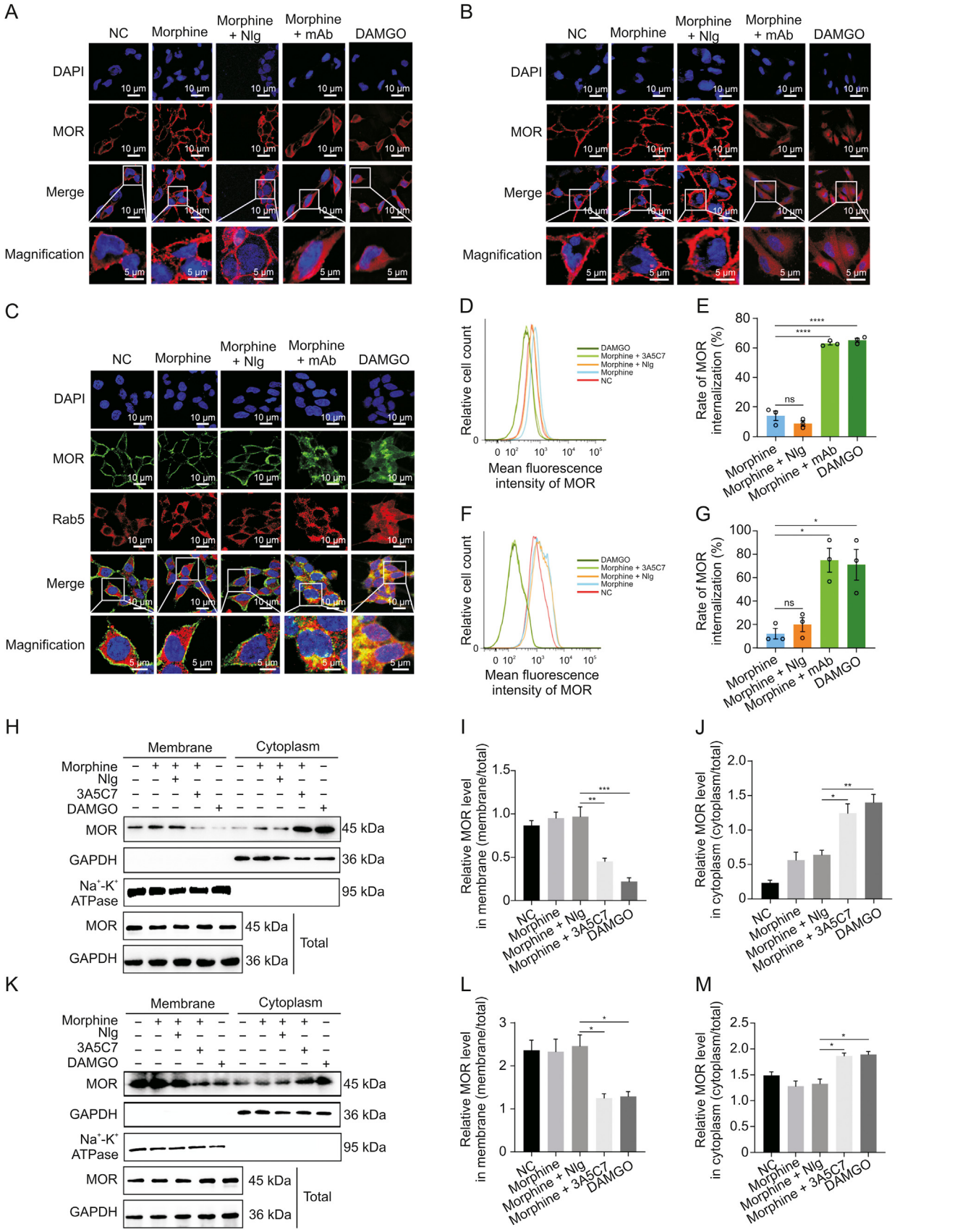

Fig. 1. Effects of 3A5C7 monoclonal antibody (mAb) on morphine-induced mu-opioid receptor (MOR) endocytosis from cell membrane to cytoplasm. (A) Immunofluorescence staining indicated the endocytosis of MOR in HEK293T-MOR cells treated with morphine and 3A5C7 mAb. (B) Immunofluorescence staining indicated the endocytosis of MOR in SH-SY5Y cells treated with morphine and 3A5C7 mAb. (C) Immunofluorescence staining manifested the colocalization of MOR and Rab5 in HEK293T-MOR cells subjected to 3A5C7 mAb and morphine. (D, E) Flow cytometry showed the endocytosis of MOR in HEK293T-MOR cells co-treated with morphine and 3A5C7 mAb. (F, G) Flow cytometry showed the

previously [27]. To estimate internalization, cells were incubated with 10 μM morphine with or without 10 μg/mL 3A5C7 mAb for 1 h at 37 °C. To measure recycling, cells were first exposed to morphine and 3A5C7 mAb for 1 h to induce internalization and then washed at 37 °C for indicated time. After internalization or recycling, cells were harvested and washed twice with ice-cold PBS by centrifugation (1000 r/min × 5 min, 4 °C), and subsequently blocked in 5% bovine serum albumin for 1 h. Detection of cell surface MOR was performed using *N*-terminal MOR antibody (AOR-011; Alomone Labs, Jerusalem, Israel) at 4 °C for 4 h. Cells were then washed twice with ice-cold PBS and incubated with fluorescein 5-isothiocyanate-conjugated secondary antibody (1:200; Invitrogen) for 1 h at 4 °C. After being washed twice with ice-cold PBS, cells were subjected to flow cytometry and analyzed using an LSR Fortessa system (BD Biosciences, San Jose, CA, USA) equipped with a 488 nm argon laser. The percentage of internalization was calculated according to the following equation: percentage of internalization = [(Negative control group − test group)/negative control group] × 100. The percentage of recycling was calculated according to the following equation: percentage of recycling = [(Recycling 15/30/60 min − recycling 0 min)/negative control group] × 100.

2.8. Stably transfected cell line construction

HEK293T cells were transfected with MOR overexpression plasmids pCI-neo-MOR (without fluorescence) and pEGFP-N1-MOR (fluorescence infusion) using lipofectamine 2000 (Thermo Fisher Scientific Inc.), and the cells were screened by 2 μg/mL puromycin for approximately 30 days after transfection. The stably transfected cell lines obtained were named HEK293T-MOR (pCI-neo-MOR transfected) and HEK293T-MOR-F (pEGFP-N1-MOR transfected), respectively.

2.9. Isolation of membrane and plasma proteins

To verify the internalization of MOR and translocation of β-arrestin2 from the plasma to the membrane, membrane and plasma proteins were extracted by a Minute™ Plasma Membrane Protein Isolation Kit (SM-005, Invent Biotechnologies, Plymouth, MN, USA) according to the manufacturer's instructions.

2.10. Immunohistochemistry

Cell immunofluorescence staining was conducted as previously described [28]. For tissue fluorescence, mice were anesthetized by isoflurane and perfused transcardially with normal saline followed by 4% paraformaldehyde (PFA). The dorsal root ganglions (DRGs) and hippocampus were removed and postfixed for 4 h at 4 °C in 4% PFA and then cryoprotected in 30% sucrose for 48 h at 4 °C. Then, the DRGs and hippocampus were cut into 20-μm thick slices and adhered to glass slides. Immunohistochemistry was carried out as previously described [29]. Anti-MOR antibody (ab10275; Abcam) and anti-Rab5 antibody (orb153348; Biorbyt) were used as primary antibodies, and Alexa 488-conjugated donkey anti-rabbit IgG and Alexa 555-conjugated donkey anti-goat IgG (Thermo Fisher Scientific Inc.) were used as secondary antibodies to detect the internalization of MOR in DRGs and the hippocampus.

2.11. Coimmunoprecipitation (co-IP)

The interaction between MOR and GRK2/β-arrestin2 was detected by co-IP assays, which were performed strictly according to the manufacturer's instructions (26,149; Thermo Fisher Scientific Inc.). Anti-MOR antibody (AOR-011; Alomone Labs), anti-GRK2 antibody, and anti-β-arrestin2 antibody were used.

2.12. Cyclic adenosine monophosphate (cAMP) accumulation assay

Cells were first exposed to morphine (10 μM) for 72 h at 37 °C to induce tolerance and then incubated with 3A5C7 mAb (10 μg/mL) for 30 min at 37 °C. Then, the cells were stimulated with 10 μM forskolin (Sigma-Aldrich) for 30 min at 37 °C. Collected cells (1.0×10^5) or tissues were disrupted by ultrasound and centrifuged at 12,000 *g* for 20 min. The protein concentration in the supernatant was detected with BCA quantification. Then, the cAMP concentration in the supernatant was determined with a cAMP ELISA kit according to the manufacturer's instructions (E-EL-0056c; Elabscience, Wuhan, China) and normalized to the protein concentration.

2.13. Intrathecal catheter implantation and drug administration

To investigate the effects of mAb 3A5C7 on the development of morphine tolerance in vivo, mice were implanted with a catheter for intrathecal injection of IgG or mAb 3A5C7 as previously described with slight modifications [30]. Mice were anesthetized with isoflurane (4% (*V*/*V*) for induction and 1.5% (*V*/*V*) for maintenance) and were placed on a surgical table in the prone position. After shaving and sterilizing the back skin, a midline longitudinal skin incision (2.0 cm) was made above L4–L6, and muscle tissues were carefully separated to expose vertebrae L4–L6 under a microscope. A polyethylene catheter (RWD Life Science Co., Ltd., Shenzhen, China) filled with normal saline was guided and slowly inserted between the L5 and L6 spinal processes at an angle of approximately 20°–30° above the vertebral column. A brisk tail-flick was observed on dura penetration. The catheter was then slowly pushed upward, parallel to the vertebral column, through the intervertebral space for approximately 1.5 cm and then fixed by suturing to the superficial muscles. Subcutaneous tissues were separated gently with forceps from the incision at the back, toward the head of the mouse, and a small longitudinal incision was made in the skin of the posterior surface over the head. Then, the other end of the catheter, which was left outside, was bent toward the head of the mouse, guided under the skin, and removed from the incision on the posterior surface over the head. Finally, this end of the catheter was fixed by suturing to the skin over the head. Mice were then placed on a heating pad and monitored until they became conscious and ambulatory.

Mice were housed individually and were allowed to recover for at least three days before drug administration and behavior tests. For chronic mAb administration, mice were injected with saline (subcutaneously, s.c.), morphine (10 mg/kg, s.c.), morphine

endocytosis of MOR in SH-SY5Y cells co-treated with morphine and 3A5C7 mAb. (H) Immunoblots showed the endocytosis of MOR in HEK293T-MOR cells co-treated with morphine and 3A5C7 mAb. 3A5C7 mAb (10 μg/mL) and morphine (10 μM) were simultaneously added to the culture media for 72 h before assay. (I, J) Quantification of relative MOR level in the cell membrane (I) and cytoplasm (J) from Fig. 1H. (K) Immunoblots showed the endocytosis of MOR in SH-SY5Y cells co-treated with morphine and 3A5C7 mAb. 3A5C7 mAb (10 μg/mL) and morphine (10 μM) were simultaneously added to the culture media for 72 h before assay. (L, M) Quantification of relative MOR level in the cell membrane (L) and cytoplasm (M) from Fig. 1K. Na^+-K^+ adenosine triphosphatase (ATPase) α1 subunit was used as internal reference of cell membrane and glyceraldehyde 3-phosphate dehydrogenase (GAPDH) was used as internal reference of cytoplasm in Figs. 1H–M. [D-Ala2, *N*-MePhe4, Gly-ol]-enkephalin (DAMGO) was used as positive controls. One-way analysis of variance with Bonferroni's post hoc tests were used for statistical analysis. Data were presented as mean ± standard error of mean ($n = 3$ independent experiments). $^*P < 0.05$, $^{**}P < 0.01$, $^{***}P < 0.001$, and $^{****}P < 0.0001$. ns: no significance. NC: negative blank control; NIg: normal IgG; DAPI: 4′,6-diamidino-2-phenylindole dihydrochloride.

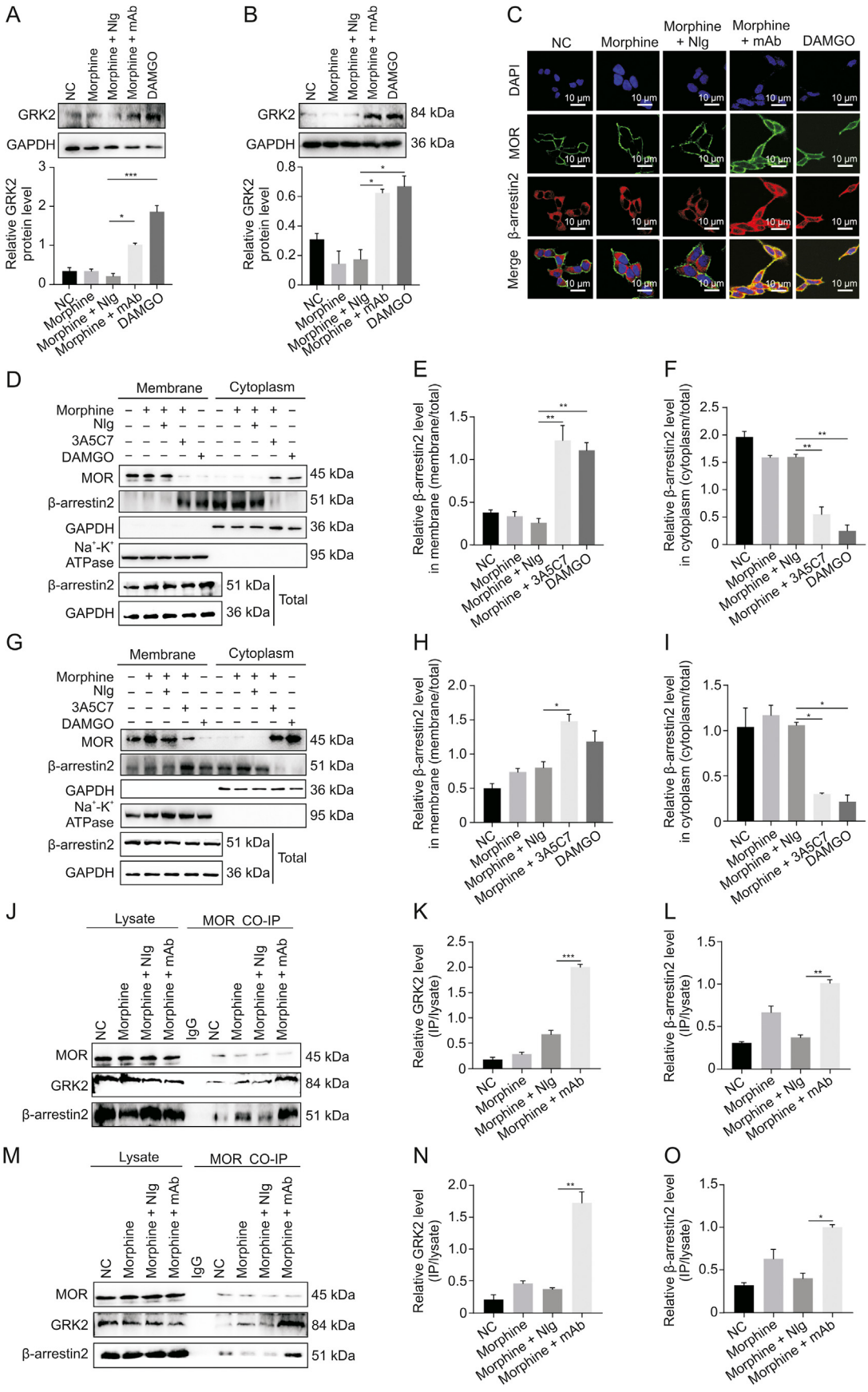

Fig. 2. 3A5C7 monoclonal antibody (mAb) regulated morphine-induced mu-opioid receptor (MOR) endocytosis through a G protein-coupled receptor kinase 2 (GRK2)/β-arrestin2-dependent way. (A) Western blot and quantification showed the upregulation of GRK2 in HEK293T-MOR cells treated with morphine and 3A5C7 mAb. (B) Western blot and

(10 mg/kg, s.c.) + IgG (4 μg, 5 μL, intrathecally, i.t.), or morphine (10 mg/kg, s.c.) + 3A5C7 mAb (4 μg, 5 μL, i.t.) once daily for 8 consecutive days. When drugs were i.t. delivered, a 10 μL microsyringe was connected to the end of the catheter on the head of the mice, and the injection was conducted over 60 s with a microinjection pump (Baoding Longer Precision Pump Co., Ltd., Baoding, China). The hotplate test was conducted once daily in the first 7 days, and the withdrawal test was performed on the 8th day after drug administration. For acute mAb administration, mice were first injected (s.c.) with morphine twice daily (9 a.m. and 5 p.m.) for 5 consecutive days with increasing doses (10 mg/kg/injection on the 1st day, 20 mg/kg/injection on the 2nd day, 30 mg/kg/injection on the 3rd day, 40 mg/kg/injection on the 4th day, and 50 mg/kg/injection on the 5th day). On the 6th day, the mice were acutely treated with saline (s.c.) + IgG (4 μg, 5 μL, i.t.), saline (s.c.) + mAb (4 μg, 5 μL, i.t.), morphine (50 mg/kg, s.c.) + IgG (4 μg, 5 μL, i.t.), or morphine (50 mg/kg, s.c.) + mAb (4 μg, 5 μL, i.t.), after which a withdrawal jumping test was performed. To investigate the effects of 3A5C7 mAb on chronic body weight loss in morphine-tolerant mice, an independent batch of mice were injected with saline (s.c.), morphine (10 mg/kg, s.c.), morphine (10 mg/kg, s.c.) + IgG (4 μg, 5 μL, i.t.), or morphine (10 mg/kg, s.c.) + 3A5C7 mAb (4 μg, 5 μL, i.t.) once daily for 10 consecutive days. The body weights of these mice were measured each day immediately before drug administration.

2.14. Intrathecal electroporation

To knockdown GRK2 and β-arrestin2, short hairpin ribonucleic acid (shRNA) was delivered into DRGs by intrathecal electroporation as previously described [31]. A double lumen catheter was constructed with two parallel polyethylene tubes (RWD Life Science Co., Ltd.), with one lumen serving as the pathway for intrathecal shRNA delivery and the other lumen serving as the pathway for the negative electrode for electroporation. The tip of the lumen, which serves as the pathway for the negative electrode, was capped with blind-end hollow fiber dialysis membrane, and a nichrome wire (0.0026″; Wire Tronic, Pine Grove, CA, USA) was passed into the lumen until this blind end.

The double lumen catheter was implanted into the intrathecal space (L2–L5) through a cisternal incision as previously described [32]. Briefly, mice were anesthetized with isoflurane and placed on a surgical table in the prone position. After shaving and sterilizing the skin on the back of the head and neck, a midline incision was made on the back of the neck, and muscles were carefully separated to expose the cisternal membrane. The cisternal membrane was opened with a stab blade and the double lumen catheter was inserted slowly through the cisternal opening, caudally into the intrathecal space of L2–L5. The catheter was fixed in place by suturing to the superficial muscles. All animals were allowed to recover for three days before subsequent experiments. Adenovirus vectors expressing *Grk2* shRNA, *Arrb2* shRNA, or control shRNA (NC) (constructed by GenePharma, Shanghai, China) were delivered (10^9 PFU in 5 μL) through one lumen of the intrathecal double lumen catheter. The nichrome wire in the other lumen was connected with a negative electrode, and a positive electrode was placed on the tail of the mice. The negative electrode and positive electrode were connected to a pulse generator (BTX Harvard Bioscience, Holliston, MA, USA). Five shocks of 200 V, with a pulse duration of 75 ms and an interval of 925 ms, were applied by the generator during isoflurane anesthesia. After three days of recovery, the anti-tolerance effects of chronic mAb administration were measured using the hotplate test as described in Section 2.13.

2.15. Hotplate test

As previously described, the effect of MOR mAb on morphine tolerance was evaluated by the hotplate test once daily during chronic mAb administration [33]. The basal latency was recorded before treatment, and a cutoff time of 30 s was set to avoid tissue damage. The analgesic effect was defined as the difference between the test latency and the basal latency (test latency − basal latency). The percentage of the maximum possible effect (MPE) was calculated according to the following equation: percentage of MPE = [(Test latency − basal latency)/(30 − basal latency)] × 100. The basal latency and test latency of each group were recorded, and the MPE was calculated daily. After the last hotplate test on the 7th day, an independent batch of mice were euthanized with excess pentobarbital without continuing to withdrawal jumping tests, and their tissue samples were collected for Western blot, immunohistochemistry, and cAMP assays.

2.16. Morphine dependence test (withdrawal jumping test)

Patients with morphine dependence experience multiple aversive behavioral and psychological symptoms once morphine is withdrawn, such as body ashes, muscle spasms, abdominal cramps, nausea/vomiting/diarrhea, insomnia, and tachycardia, which are collectively referred to as opioid withdrawal syndrome (OWS) [34]. Noticeably, fear of and escape from OWS contribute to the maintenance of drug-taking and the failure of morphine discontinuation in morphine-dependent individuals, serving as a negative reinforcer to enhance morphine dependence [35]. Among the symptoms of OWS, jumping precipitated by the MOR antagonist naloxone is considered as the most sensitive and reliable index of withdrawal intensity after both chronic and acute morphine exposure in rodents and is also a commonly used behavior paradigm to reflect dependence [36]. Thus, we harnessed the naloxone-precipitated withdrawal jumping test to investigate the effects of the 3A5C7 mAb on morphine dependence.

The naloxone-precipitated withdrawal jumping test was performed after chronic mAb and acute mAb administration as mentioned above (Section 2.13) according to a previous study [37]. Two hours after the last morphine administration in both chronic and acute mAb procedures, 1 mg/kg naloxone was injected (s.c.) to mice. Mice were immediately placed in transparent acrylic boxes (32.7 cm wide × 12.6 cm long × 37.7 cm high) and were closely

quantification showed the upregulation of GRK2 in SH-SY5Y cells treated with morphine and 3A5C7 mAb. (C) Immunofluorescence staining showed the translocation of β-arrestin2 from cytoplasm to cell membrane in HEK293T-MOR cells treated with morphine and 3A5C7 mAb. (D) Immunoblots showed the translocation of β-arrestin2 from cytoplasm to cell membrane in HEK293T-MOR cells treated with morphine and 3A5C7 mAb. (E, F) Quantification of relative β-arrestin2 level in the cell membrane (E) and cytoplasm (F) from Fig. 2D. (G) Immunoblots showed the translocation of β-arrestin2 from cytoplasm to cell membrane in SH-SY5Y cells treated with morphine and 3A5C7 mAb. (H, I) Quantification of relative β-arrestin2 level in the cell membrane (H) and cytoplasm (I) from Fig. 2G. (J) Coimmunoprecipitation (Co-IP) assay demonstrated the interaction of MOR with GRK2 and β-arrestin2 after treatment with morphine and 3A5C7 mAb in HEK293T-MOR cells. (K, L) Quantification of the relative levels of GRK2 and β-arrestin2 interacting with MOR from Fig. 2J. (M) Co-IP assay demonstrated the interaction of MOR with GRK2 and β-arrestin2 after treatment with morphine and 3A5C7 mAb in SH-SY5Y cells. (N, O) Quantification of the relative levels of GRK2 and β-arrestin2 interacting with MOR from Fig. 2M. Na^+-K^+ adenosine triphosphatase (ATPase) α1 subunit was used as internal reference of cell membrane and glyceraldehyde 3-phosphate dehydrogenase (GAPDH) was used as internal reference of cytoplasm. [D-Ala2, *N*-MePhe4, Gly-ol]-enkephalin (DAMGO) was used as positive controls. One-way analysis of variance with Bonferroni's post hoc tests were used for statistical analysis. Data were presented as mean ± standard error of mean ($n = 3$ independent experiments). $^*P < 0.05$, $^{**}P < 0.01$, and $^{***}P < 0.001$. NC: negative blank control; Nlg: normal IgG; DAPI: 4′,6-diamidino-2-phenylindole dihydrochloride.

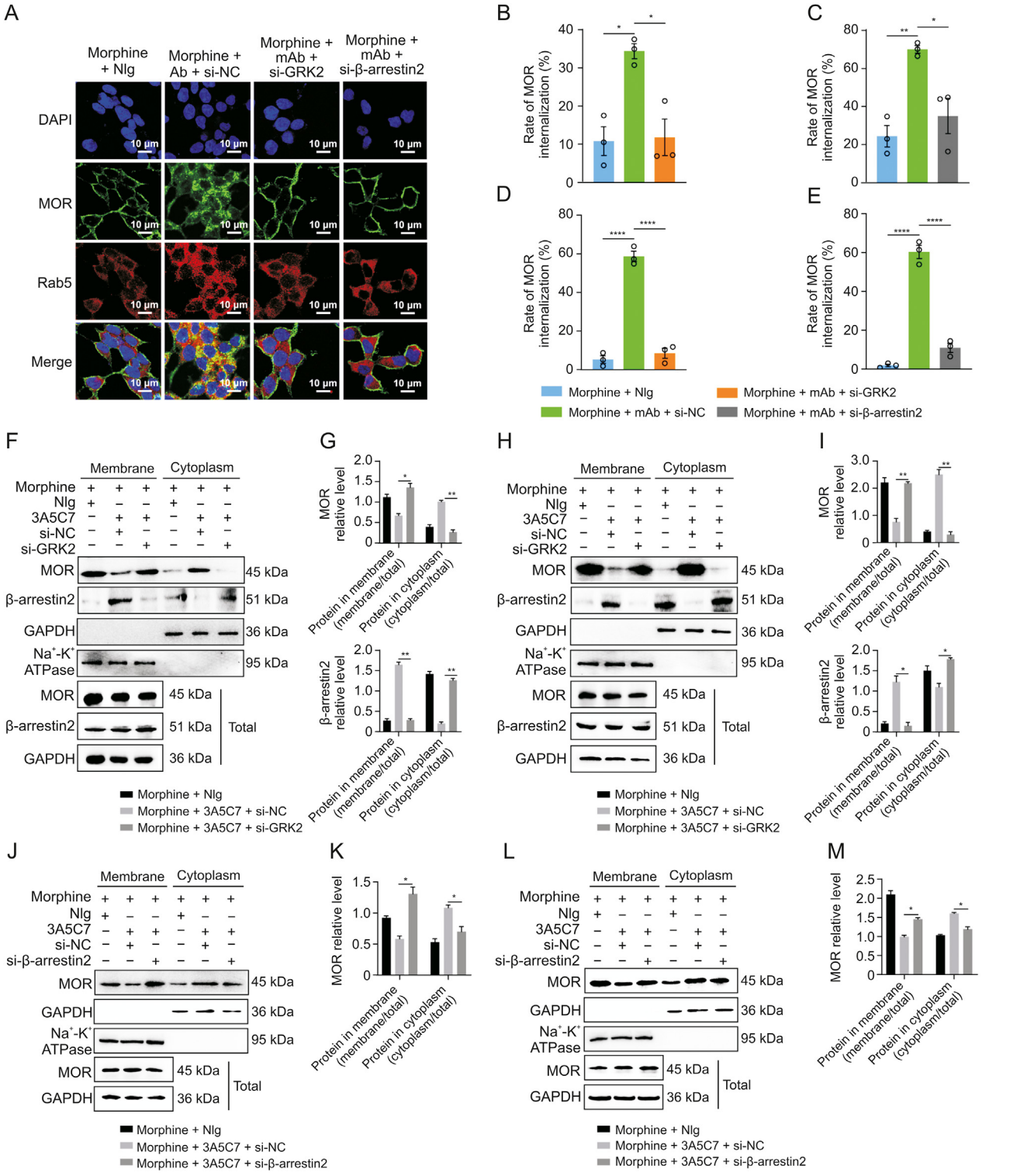

Fig. 3. Effects of G protein-coupled receptor kinase 2 (GRK2) and β-arrestin2 knockdown on the endocytosis of mu-opioid receptor (MOR) induced by morphine and 3A5C7 monoclonal antibody (mAb). (A) Immunofluorescence staining showed that the MOR endocytosis induced by morphine and 3A5C7 mAb was reduced in HEK293T-MOR cells with GRK2 or β-arrestin2 knockdown. (B, C) Flow cytometry indicated that MOR endocytosis induced by morphine and 3A5C7 mAb was reduced in HEK293T-MOR cells with GRK2 (B) or β-arrestin2 knockdown (C). (D, E) Flow cytometry indicated that MOR endocytosis induced by morphine and 3A5C7 mAb was reduced in SH-SY5Y cells with GRK2 (D) or β-arrestin2 (E) knockdown. (F) Immunoblots showed that GRK2 knockdown reduced MOR endocytosis and translocation of β-arrestin2 from cytoplasm to cell membrane in HEK293T-MOR cells. (G) Quantification of the relative levels of MOR and β-arrestin2 in the membrane and cytoplasm from Fig. 3F. (H) Immunoblots showed that GRK2 knockdown reduced MOR endocytosis and translocation of β-arrestin2 from cytoplasm to cell membrane in SH-SY5Y cells. (I) Quantification of the relative levels of MOR and β-arrestin2 in the membrane and cytoplasm from Fig. 3H. HEK293T-MOR and SH-SY5Y cells were transfected with small interfering ribonucleic acid (siRNA) for GRK2 (si-GRK2), β-arrestin2 (si-β-arrestin2), or control siRNA (si-NC) for 48 h, co-cultured with morphine and 3A5C7 mAb/normal IgG (Nlg) for another 72 h, then cell membrane and plasma proteins were extracted and subjected to Western blot analysis. (J) Immunoblots showed that downregulation of β-arrestin2 reduced endocytosis of MOR induced by morphine and 3A5C7 mAb in HEK293T-MOR cells. (K) Quantification of the relative levels of MOR in the membrane and cytoplasm from Fig. 3J. (L) Immunoblots showed that downregulation of β-arrestin2 reduced endocytosis of MOR induced by morphine and 3A5C7 mAb in SH-SY5Y cells. (M) Quantification of the relative levels of MOR in the membrane and cytoplasm from Fig. 3L. Na^+-K^+ adenosine triphosphatase (ATPase) α1 subunit was used as internal reference of cell membrane and glyceraldehyde 3-phosphate dehydrogenase (GAPDH) was used as

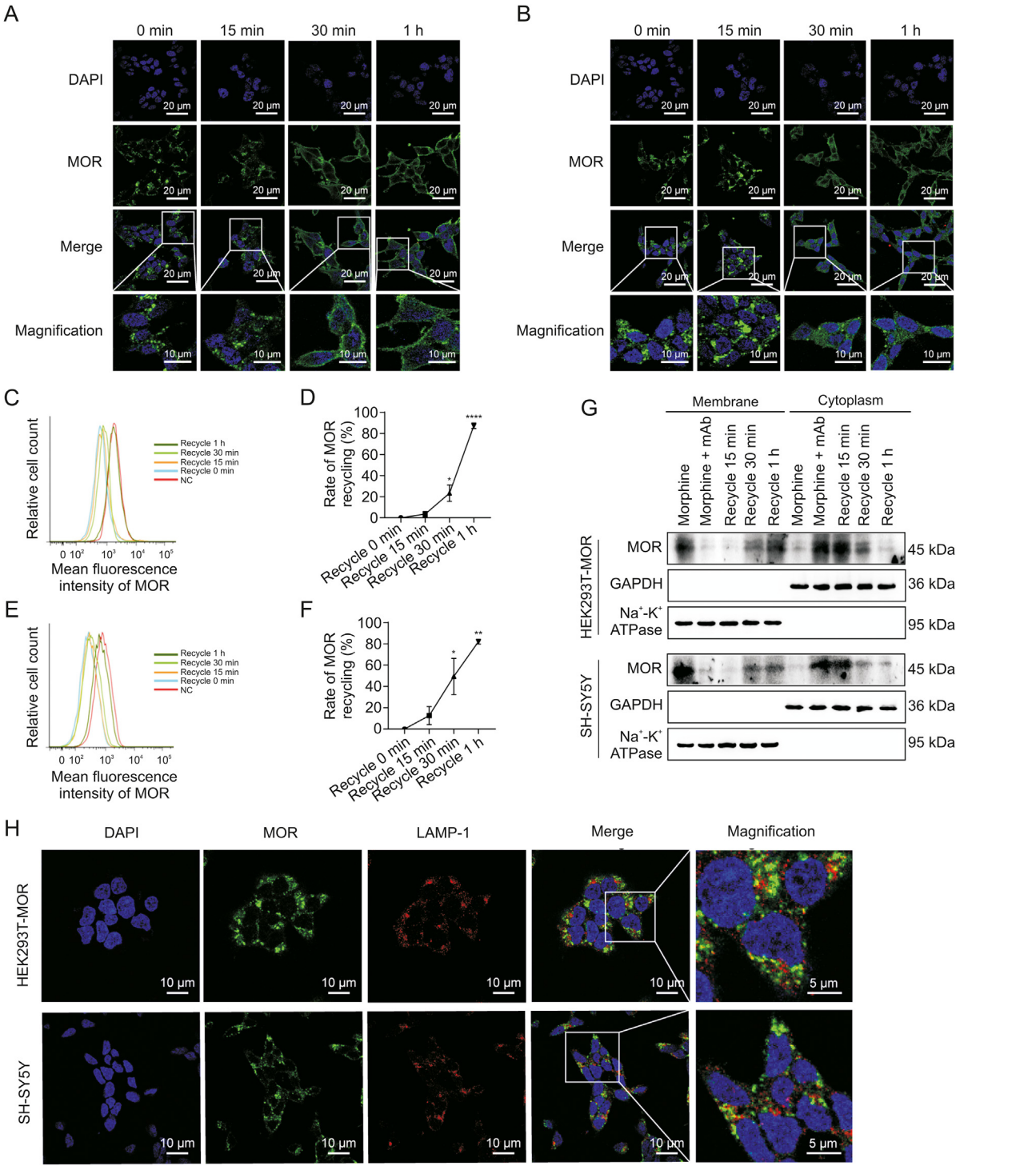

Fig. 4. Effects of 3A5C7 monoclonal antibody (mAb) on mu-opioid receptor (MOR) recycling from cytoplasm to cell membrane. (A) Immunofluorescence staining of HEK293T-MOR cells to demonstrate the recycling of MOR. (B) Immunofluorescence staining of SH-SY5Y cells to demonstrate the recycling of MOR. (C, D) Flow cytometry demonstrating the recycling of MOR in HEK293T-MOR cells (C) and corresponding quantification as percentages of control cell surface MOR without any treatment (D). (E, F) Flow cytometry demonstrating the recycling of MOR in SH-SY5Y cells (E) and corresponding quantification as percentages of control cell surface MOR without any treatment (F). HEK293T-MOR or SH-SY5Y cells were exposed to morphine (10 μM) and 3A5C7 (10 μg/mL) for 1 h to induce internalization which were washed out thereafter. MOR recycling was monitored at 0 min, 15 min, 30 min, and 1 h after washout. (G) Western blot showed the MOR recycling from cytoplasm to cell membrane. HEK293T-MOR or SH-SY5Y cells were treated as indicated and cell membrane and plasma proteins were extracted for assays. (H) Immunofluorescence staining showed the relationship between internalized MOR and lysosome associated membrane protein-1 (LAMP-1), the marker of lysosome. Cells were treated with morphine and 3A5C7 mAb for 1 h at 37 °C before assay. Na^+-K^+ adenosine triphosphatase (ATPase) α1 subunit was used as internal reference of cell membrane and glyceraldehyde 3-phosphate dehydrogenase (GAPDH) was used as internal reference of cytoplasm. Student's *t* tests were used for statistical analysis. Data were presented as mean ± standard error of mean ($n = 3$ independent experiments). $^{*}P < 0.05$, $^{**}P < 0.01$, and $^{****}P < 0.0001$ versus recycle 0 min in Figs. 4D and F. DAPI: 4′,6-diamidino-2-phenylindole dihydrochloride; NC: negative blank control.

internal reference of cytoplasm. One-way analysis of variance with Bonferroni's post hoc tests were used for statistical analysis. Data were presented as mean ± standard error of mean ($n = 3$ independent experiments). $^{*}P < 0.05$, $^{**}P < 0.01$, $^{***}P < 0.001$, and $^{****}P < 0.0001$. DAPI: 4′,6-diamidino-2-phenylindole dihydrochloride.

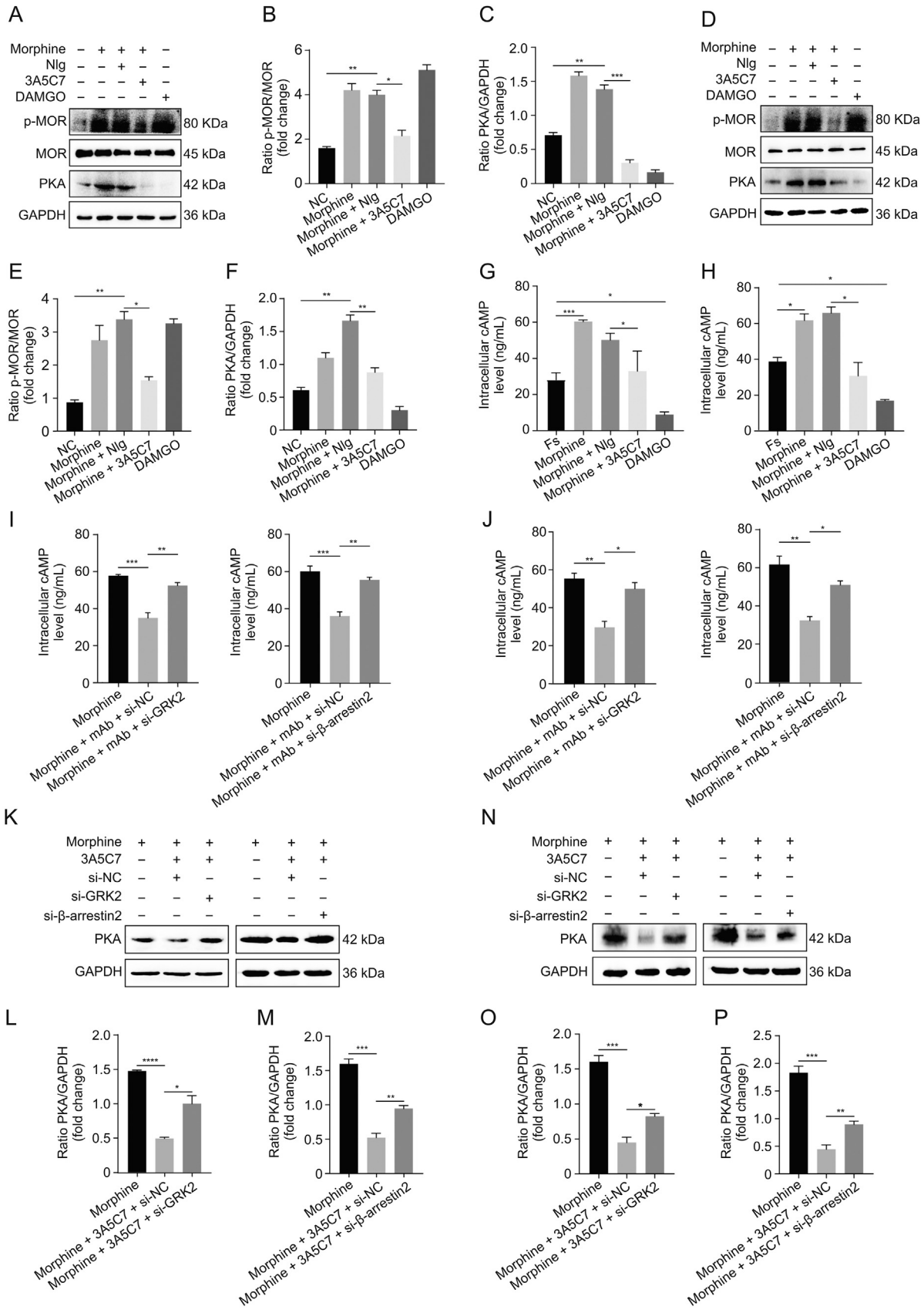

Fig. 5. 3A5C7 monoclonal antibody (mAb) attenuates morphine tolerance in vitro. (A) Immunoblots showed the inhibitory effects of 3A5C7 mAb on morphine-induced upregulation of phospho-MOR (p-MOR) Serine 375 and protein kinase A (PKA) in HEK293T-MOR cells. (B) Quantification of the level of p-MOR in Fig. 5A. (C) Quantification of the level of PKA in Fig. 5A. (D) Immunoblots showed the inhibitory effects of 3A5C7 mAb on morphine-induced upregulation of p-MOR Serine 375 and PKA in SH-SY5Y cells. (E) Quantification of the level of p-MOR in Fig. 5D. (F) Quantification of the level of PKA in Fig. 5D. (G) The effects of 3A5C7 mAb on the level of intracellular cyclic adenosine monophosphate (cAMP) in

monitored. The number of jumps, defined as simultaneous removal of all four paws from the horizontal bottom surface, was counted by an investigator blinded to the experimental groups in the following 30 min. Before naloxone administration, mice were placed in acrylic boxes for 30 min to acclimate to the environment. For naloxone administration, mice were briefly removed from the boxes to receive naloxone injection and were immediately returned back to the boxes. Boxes were cleaned between tests with 75% (*V*/*V*) ethanol to erase the odors of different mice.

2.17. Statistical analysis

All in vitro experiments were repeated independently at least three times. All data are presented as the mean ± standard error of mean (SEM). Two groups were compared using Student's *t*-test. Multiple groups were compared using one-way analysis of variance (ANOVA) or two-way ANOVA with Bonferroni's post hoc tests. Statistical analysis was performed with GraphPad Prism v8.0 (GraphPad Software, Boston, MA, USA). $P < 0.05$ was considered to be statistically significant.

3. Results

3.1. Cell model of morphine tolerance in vitro

To develop an available cell model for our subsequent in vitro experiments, we induced the differentiation of the human neuroblastoma cell line SH-SY5Y using RA, which displays opioid tolerance by upregulating the adenylate cyclase (AC) effector system [38]. Western blot analysis showed that MOR is overexpressed in undifferentiated SH-SY5Y cells compared with U87MG and U251 nerve cell lines (Fig. S3A). After induction by RA for 6 days, SH-SY5Y cells differentiated into neuronal-like cells (Fig. S3B), displaying neuronal characteristics of smaller soma, fusiform or polygon forms, long neurites, and proliferation reduction. Moreover, the differentiation of SH-SY5Y cells was confirmed by a significant increase in the release of LDH, a marker of SH-SY5Y cell differentiation [38] (Fig. S3C). These results demonstrated that differentiated SH-SY5Y cell model was successfully established and could be applied to the following experiments.

3.2. MAb targeting MOR augments morphine-induced MOR endocytosis

Therapeutic mAb targeting GPCRs may facilitate the internalization of the targeted GPCR [39]. To test the possibility that morphine-induced MOR internalization could be initiated and promoted by mAb, we prepared and identified a specific mAb against MOR, named 3A5C7 according to the clone number, using the hybridoma technique in our lab (National Invention Patent CN113373118A; please also refer to the Section 2 and Figs. S1 and S2). Coomassie blue staining of reduced and non-reduced 3A5C7 mAb suggested that the 3A5C7 mAb belonged to the IgG subtype (Fig. S4A). Western blot of unrelated peptide (cluster of differentiation 147, CD147), cells overexpressing MOR (HEK293T-MOR), and cells with MOR knockdown (SH-SY5Y si-MOR) displayed the good specificity of the 3A5C7 mAb (Fig. S4B). In addition, cellular ELISA (Fig. S4C) and ITC tests (Figs. S4D and E) showed that the 3A5C7 mAb had good affinity. Furthermore, immunofluorescence staining (Fig. S4F) and flow cytometry assays (Figs. S4G and H) demonstrated that the 3A5C7 mAb also had the ability to bind to the MOR antigen with spatial conformation. Finally, DNA sequencing was performed to determine the variable region gene sequences on the heavy and light chains of the 3A5C7 mAb, and the corresponding sequences are shown in Figs. S4I and J. Taken together, these results suggested that the 3A5C7 mAb had good affinity and specificity to MOR antigen with or without spatial conformation, which laid the groundwork for the following functional investigations using this mAb.

Immunofluorescence staining showed that the 3A5C7 mAb significantly augmented morphine-induced MOR endocytosis in HEK293T-MOR (Fig. 1A) and SH-SY5Y (Fig. 1B) cells, whereas morphine or morphine plus control IgG (normal IgG, NIg) had no such effect. DAMGO-induced internalization was used as positive controls. Consistently, the 3A5C7 mAb also promoted morphine-induced MOR endocytosis in HEK293T-MOR-F cells (Fig. S5A). Endocytosis of plasma membrane receptors is regulated by the Rab family, especially Rab5, a marker of early endosomes involved in endocytosis of GPCRs [27]. We observed the colocalization of endocytosed MOR and Rab5 in HEK293T-MOR cells cotreated with morphine and 3A5C7 mAb (Fig. 1C). Flow cytometry analysis validated the endocytosis of MOR in the cotreatment of morphine and 3A5C7 mAb (Figs. 1D–G). Finally, Western blot further confirmed the simultaneous decrease of MOR on the cell membrane and the increase in the cytoplasm when cells were exposed to morphine plus 3A5C7 mAb compared to cells exposed to morphine plus NIg in both HEK293T-MOR (Figs. 1H–J) and SH-SY5Y cells (Figs. 1K–M). Interestingly, 3A5C7 mAb alone could not promote MOR internalization without morphine (Figs. S5B, S6A, and S6B). Taken together, these results indicated that the 3A5C7 mAb could potentiate the morphine-induced endocytosis of MOR in vitro.

3.3. MAb targeting MOR promotes morphine-induced MOR endocytosis through a GRK2/β-arrestin2-dependent mechanism

We next investigated the mechanism underlying mAb-facilitated MOR internalization. It was reported that morphine-induced MOR endocytosis was mediated by the GRK2/β-arrestin2 pathway [34]. We found that the protein level of GRK2 was upregulated (Figs. 2A and B) and that β-arrestin2 was translocated from the cytoplasm to the plasma membrane (Figs. 2C–I) in cells cotreated with morphine and 3A5C7 mAb. However, 3A5C7 mAb alone neither changed the expression of GRK2 nor promoted the translocation of β-arrestin2 (Fig. S6). Then, co-IP assays indicated that cotreatment with morphine and 3A5C7 mAb increased the amount of GRK2 and β-arrestin2 pulled down by MOR in HEK293T-MOR (Figs. 2J–L) and SH-SY5Y (Figs. 2M–O) cells compared to

HEK293T-MOR cells. (H) The effects of 3A5C7 mAb on the level of intracellular cAMP in SH-SY5Y cells. Cells were subjected to morphine and 3A5C7 antibody for 72 h, then treated with forskolin (Fs, 10 μM) for 30 min at 37 °C. Enzyme-linked immunosorbent assay (ELISA) was conducted to determine the concentration of cAMP. Forskolin-stimulated cAMP level was used as the basal value. (I) The influences of G protein-coupled receptor kinase 2 (GRK2) and β-arrestin2 knockdown on the inhibitory effects of 3A5C7 on morphine-induced increase in intracellular cAMP in HEK293T-MOR cells. (J) The influences of GRK2 and β-arrestin2 knockdown on the inhibitory effects of 3A5C7 on morphine-induced increase in intracellular cAMP in SH-SY5Y cells. (K) Immunoblots showing the influences of GRK2 and β-arrestin2 knockdown on the inhibitory effects of 3A5C7 on morphine-induced increase in PKA in HEK293T-MOR cells. (L, M) Quantification of the relative expression levels of PKA in Fig. 5K. (N) Immunoblots showing the influences of GRK2 and β-arrestin2 knockdown on the inhibitory effects of 3A5C7 on morphine-induced increase in PKA in SH-SY5Y cells. (O, P) Quantification of the relative expression levels of PKA in Fig. 5N. [D-Ala2, *N*-MePhe4, Gly-ol]-enkephalin (DAMGO) was used as positive controls. One-way analysis of variance with Bonferroni's post hoc tests were used for statistical analysis. Data were presented as mean ± standard error of mean ($n = 3$ independent experiments). $^{*}P < 0.05$, $^{**}P < 0.01$, $^{***}P < 0.001$, and $^{****}P < 0.0001$. NIg: normal IgG; GAPDH: glyceraldehyde 3-phosphate dehydrogenase; NC: negative blank control; si-GRK2: small interfering RNA (siRNA) for GRK2; si-β-arrestin2: siRNA for β-arrestin2; si-NC: control siRNA.

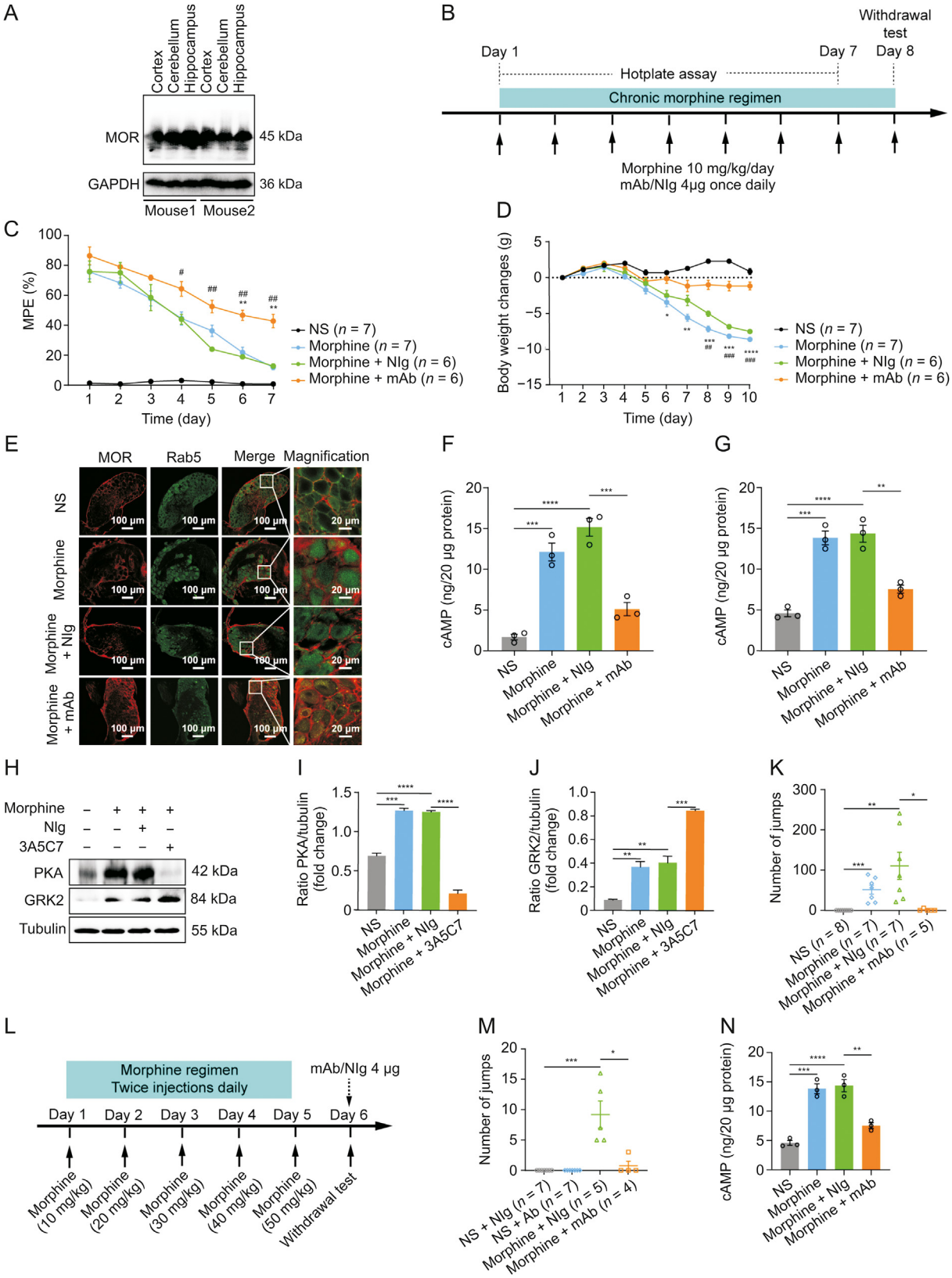

Fig. 6. 3A5C7 monoclonal antibody (mAb) attenuates morphine antinociceptive tolerance and physical dependence in mice. (A) Western blots indicating the cross specificity of 3A5C7 mAb against mu-opioid receptor (MOR) in the cortex, cerebellum, and hippocampus from C57/B6 mice. (B) Experiment flowchart for testing the effects of chronically administered 3A5C7 mAb on morphine tolerance and dependence. (C) The effects of chronically administered 3A5C7 mAb on the antinociceptive effects of morphine in mice measured by hotplate test. (D) The body weight changes of morphine-tolerant mice. Two-way analysis of variance with Bonferroni's post hoc tests were used for statistical analysis (n = 6–7 mice in each group). $^{*}P < 0.05$, $^{**}P < 0.01$, $^{***}P < 0.001$, and $^{****}P < 0.0001$, morphine + mAb group vs. morphine group. $^{\#}P < 0.05$, $^{\#\#}P < 0.01$, and $^{\#\#\#}P < 0.001$, morphine + mAb group vs. morphine + normal IgG (NIg) group. (E) Representative immunofluorescence staining of MOR and Rab5 in the mouse dorsal root ganglions (DRGs) after

treatment with morphine and NIg. Therefore, we speculated that GRK2 and β-arrestin2 played a crucial role in mAb-facilitated morphine-induced MOR endocytosis. To further explore the function of GRK2 and β-arrestin2 in MOR endocytosis, the expression levels of GRK2 and β-arrestin2 were knocked down in HEK293T-MOR and SH-SY5Y cells by siRNA, which was confirmed by real-time PCR and Western blot assays (Figs. S7A–F). In HEK293T-MOR cells, immunofluorescence staining showed that MOR endocytosis induced by morphine combined with the 3A5C7 mAb was significantly decreased after GRK2/β-arrestin2 was knocked down (Fig. 3A), which was verified by flow cytometry (Figs. 3B–E and S7G–J) and Western blot (Figs. 3F–M). Interestingly, it was also found that the translocation of β-arrestin2 from the cytoplasm to the membrane was disrupted when GRK2 was knocked down by siRNA (Figs. 3F–I and S7K), indicating that GRK2 was upstream of β-arrestin2 in the regulation of MOR endocytosis. Taken together, these results suggested that the 3A5C7 mAb enhanced morphine-induced MOR endocytosis in a GRK2/β-arrestin2-dependent manner.

3.4. MAb targeting MOR allows recycling of MOR back to the cell surface

Recycling of internalized MOR to the plasma membrane helps to resensitize the function of MOR [22,27]. We then examined whether 3A5C7 mAb had effects on the recycling of MOR by removing mAb and morphine after internalization. Immunofluorescence staining showed that MOR started to recycle back to the cell surface at 30 min and completely recycled back to the plasma membrane at 1 h after 3A5C7 mAb and morphine was washed out in HEK293T-MOR and SH-SY5Y cells (Figs. 4A and B), which was confirmed by flow cytometry and Western blot assays (Figs. 4C–G). Monensin, the recycling inhibitor, diminished MOR recycling after mAb and morphine washout (Figs. S8A and B). In addition, immunofluorescence staining showed that internalized MOR did not colocalize with the LAMP-1, a marker of lysosomes, suggesting that internalized MOR would not undergo degradation in lysosomes (Fig. 4H). These findings demonstrated that the 3A5C7 mAb did not interfere with the recycling of MOR after internalization.

3.5. MAb targeting MOR reduces morphine tolerance by promoting MOR endocytosis in vitro

Next, we explored whether 3A5C7 mAb-induced enhancement of MOR endocytosis could alleviate morphine tolerance in vitro. Serine 375 (S375) of MOR is the primary phosphorylation site that contributes to MOR desensitization in morphine tolerance [19]. We observed that the 3A5C7 mAb attenuated morphine-induced phosphorylation at S375 of MOR in HEK293T-MOR (Figs. 5A–C) and SH-SY5Y (Figs. 5D–F) cells without affecting the expression level of MOR. Meanwhile, the 3A5C7 mAb itself did not change the p-MOR (S375) level (Figs. S8C and D). Hyperactivation of AC and the resultant rise in cAMP and PKA are molecular markers of morphine tolerance in vitro [40]. Here, Western blot (Figs. 5A–F) and ELISA (Figs. 5G and H) showed that the 3A5C7 mAb could inhibit morphine-induced cAMP accumulation and PKA upregulation, suggesting that AC hyperactivation was suppressed by the 3A5C7 mAb. The 3A5C7 mAb itself did not affect PKA levels (Figs. S6C and D). Moreover, siRNA-induced knockdown of GRK2 or β-arrestin2 reversed cAMP (Figs. 5I and J) and PKA (Figs. 5K–P) inhibition induced by 3A5C7 mAb compared to control siRNA. These results provided in vitro evidence that the 3A5C7 mAb alleviated morphine tolerance by promoting GRK2/β-arrestin2-dependent MOR endocytosis.

3.6. 3A5C7 mAb attenuates morphine tolerance and physical dependence in mice

Next, we examined the therapeutic effects of the 3A5C7 mAb on morphine tolerance in mice. Considering that the 3A5C7 mAb was developed based on antigens of human MOR, we first tested the cross specificity of the 3A5C7 mAb to recognize MOR from mouse species. Western blot showed that the 3A5C7 mAb could finely recognize MOR in protein samples of the cerebral cortex, cerebellum, and hippocampus from C57/B6 mice (Fig. 6A), confirming the feasibility of the 3A5C7 mAb to antagonize MOR in mice. To assess the effect of 3A5C7 mAb on morphine tolerance in terms of antinociception, hotplate tests were performed during chronic treatment with morphine and 3A5C7 mAb as shown in Fig. 6B. The MPE gradually decreased during the 7-day trial period (Fig. 6C), indicating the development of morphine tolerance in antinociception. However, mice receiving 3A5C7 mAb + morphine had significantly higher MPE from the 4th day to the 7th day compared with mice receiving NIg + morphine, and in the last two days compared with mice merely receiving morphine (Fig. 6C), suggesting that 3A5C7 mAb attenuated morphine tolerance in vivo. Body weight loss is reported to be associated with tolerance induced by chronic morphine administration [41]. We investigated the effects of 3A5C7 mAb on body weight in mice receiving repeated morphine for 10 consecutive days, and we found that the 3A5C7 mAb significantly attenuated body weight loss (Fig. 6D). Taken together, these results indicated that the 3A5C7 mAb could attenuate morphine tolerance in mice.

We further investigated whether the 3A5C7 mAb also facilitated MOR endocytosis in vivo as it did in vitro. Immunofluorescence staining demonstrated that the 3A5C7 mAb induced more MOR endocytosis in neurons of the DRGs and hippocampus (Figs. 6E and S9A) in morphine-tolerant mice. In addition, morphine-tolerant mice receiving mAb 3A5C7 had significantly decreased levels of cAMP in the cortex and hippocampus (Figs. 6F and G) and lower levels of PKA and higher levels of GRK2 in the hippocampus (Figs. 6H–J). These results confirmed that the 3A5C7 mAb could facilitate morphine-induced MOR endocytosis in vivo. The development of morphine physical dependence, characterized by naloxone-precipitated withdrawal jumping behavior, was also tested after chronic morphine treatment (Fig. 6B). Chronic morphine (s.c.) and 3A5C7 mAb (i.t.) coadministration significantly reduced the number of withdrawal jumps compared with mice treated with chronic morphine and control IgG (Fig. 6K). Next, we tested whether acute i.t. administration of 3A5C7 mAb also alleviated physical dependence after chronic morphine exposure (Fig. 6L). 3A5C7 mAb i.t. administered at the end of chronic morphine treatment was demonstrated to induce a significant reduction in naloxone-induced jumping

chronic 3A5C7 treatment ($n = 3$ mice in each group). (F) Cyclic adenosine monophosphate (cAMP) levels of cortex in mice from each treatment group ($n = 3$ mice in each group). (G) The level of cAMP of hippocampus in mice from each treatment group ($n = 3$ mice in each group). (H) Immunoblots showing the protein levels of protein kinase A (PKA) and G protein-coupled receptor kinase 2 (GRK2) in hippocampus of mice from each treatment ($n = 3$ mice in each group). (I) Quantification of the levels of PKA in Fig. 6H. (J) Quantification of the levels of GRK2 in Fig. 6H. (K) Chronic 3A5C7 mAb administration diminished naloxone-precipitated withdrawal jumping in mice ($n = 5–8$ mice in each group). (L) Experiment flowchart determining the acute effects of 3A5C7 mAb on naloxone-precipitated withdrawal jumping in morphine-tolerant mice. (M) Acute mAb administration diminished morphine withdrawal ($n = 4–7$ mice in each group). (N) cAMP concentrations of striatum in mice from each treatment ($n = 3$ mice in each group). One-way analysis of variance with Bonferroni's post hoc tests were used for statistical analysis in Figs. 6F, G, I–K, M, and N. $^{*}P < 0.05$, $^{**}P < 0.01$, $^{***}P < 0.001$, and $^{****}P < 0.0001$. Data were presented as mean ± standard error of mean. GAPDH: glyceraldehyde 3-phosphate dehydrogenase; MPE: maximum possible effect; NS: normal saline.

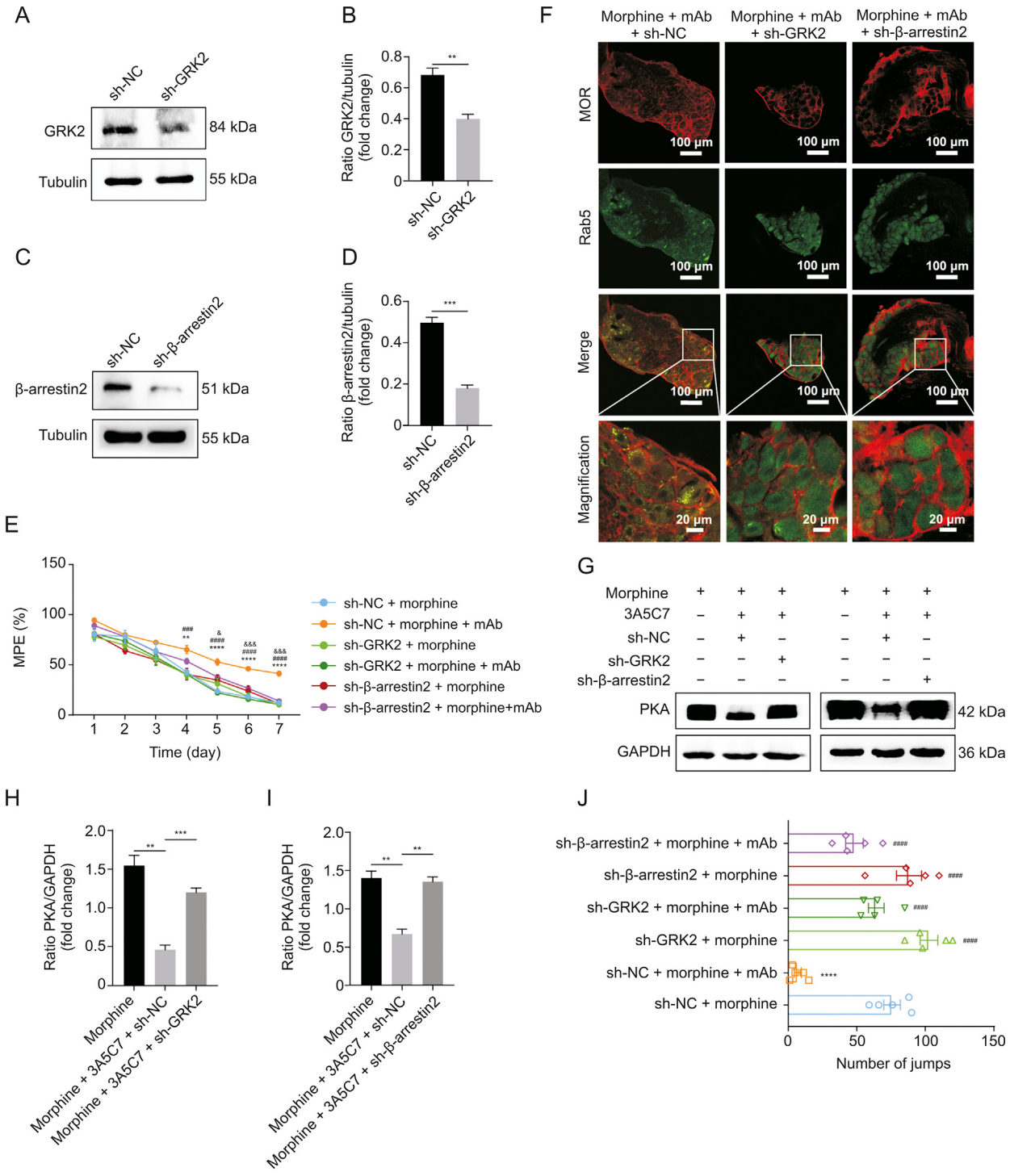

Fig. 7. 3A5C7 monoclonal antibody (mAb) attenuates morphine antinociceptive tolerance via G protein-coupled receptor kinase 2 (GRK2)/β-arrestin2 pathway in mice. (A) Immunoblot showing that GRK2 was knocked-down by short hairpin ribonucleic acid (shRNA) in dorsal root ganglions (DRGs). (B) Quantification of the protein level of GRK2 in Fig. 7A. (C) Immunoblot showing that β-arrestin2 was knocked-down by shRNA in DRGs. (D) Quantification of the protein level of β-arrestin2 in Fig. 7C. (E) Hotplate tests demonstrating the effects of GRK2 or β-arrestin2 knockdown on the anti-tolerance efficacy of mAb 3A5C7. Two-way analysis of variance (ANOVA) with Bonferroni's post hoc tests were used for statistical analysis. $^{**}P < 0.01$ and $^{****}P < 0.0001$, sh-NC + morphine + mAb group vs. sh-NC + morphine group; $^{\#\#\#}P < 0.001$ and $^{\#\#\#\#}P < 0.0001$, sh-NC + morphine + mAb group vs. sh-GRK2 + morphine + mAb group; $^{\&}P < 0.05$ and $^{\&\&\&}P < 0.001$, sh-NC + morphine + mAb group vs. sh-β-arrestin2 + morphine + mAb group ($n = 5$ mice in each group). (F) Representative immunofluorescence images of MOR and Rab5 for each treatment in mouse DRGs ($n = 3$ mice in each group). (G) The protein levels of hippocampal protein kinase A (PKA) from mice in each treatment group. (H, I) Quantification of the relative protein levels of PKA from Fig. 7G. One-way ANOVA with Bonferroni's post hoc tests were used for statistical analysis. $^{**}P < 0.01$ and $^{***}P < 0.001$. (J) Inhibitory effects of acute 3A5C7 mAb administration on naloxone-precipitated withdrawal jumping were reduced in GRK2- and β-arrestin2-knockdown mice. One-way ANOVA with Bonferroni's post hoc tests were used for statistical analysis. $^{****}P < 0.0001$ vs. sh-NC + morphine group; $^{\#\#\#\#}P < 0.0001$ vs. sh-NC + morphine + mAb group ($n = 5$ mice in each group). Data were presented as the mean ± standard error of mean. sh-NC: control shRNA; sh-GRK2: shRNA for GRK2; sh-β-arrestin2: shRNA for β-arrestin2; MPE: maximum possible effect; GAPDH: glyceraldehyde 3-phosphate dehydrogenase.

behavior (Fig. 6M), and significantly decreased the levels of cAMP in the striatum compared with mice receiving morphine and control IgG (Figs. 6N and S9B). These results indicated that acute 3A5C7 mAb administration had similar efficacy as chronic mAb administration in attenuating morphine dependence. Collectively, these results demonstrated that chronic mAb cotreatment with morphine alleviated the development of morphine tolerance and physical dependence and enhanced morphine-induced MOR endocytosis in vivo, while acute mAb administration at the time of morphine withdrawal could exert instant therapeutic efficacy to alleviate withdrawal symptoms.

3.7. 3A5C7 mAb attenuates morphine tolerance by facilitating MOR endocytosis in the DRG through the GRK2/β-arrestin2 pathway in mice

The above in vitro studies demonstrated that the 3A5C7 mAb attenuated morphine tolerance by enhancing morphine-induced MOR endocytosis in a GRK2/β-arrestin2-dependent manner. We next investigated whether this complies with the therapeutic effects of mAb on morphine tolerance in vivo. Intrathecal electroporation of shRNA silenced either GRK2 or β-arrestin2 in DRG neurons in vivo (Figs. 7A–D). Silencing of GRK2 or β-arrestin2 did not influence the basal nociceptive sensitivity of mice, but reduced the enhancement effects of chronic 3A5C7 mAb administration on morphine analgesia (Fig. 7E). MOR endocytosis (Fig. 7F), and the inhibition of AC hyperactivation (Figs. 7G–I) were abolished after GRK2 or β-arrestin2 knockdown, suggesting that GRK2 and β-arrestin2 were involved in the chronic therapeutic effects of 3A5C7 mAb on morphine tolerance in vivo. Similarly, the attenuation of withdrawal behavior by acute 3A5C7 mAb administration was also reversed in GRK2/β-arrestin2 silenced mice (Fig. 7J). Taken together, these results suggested that the 3A5C7 mAb attenuated morphine tolerance and physical dependence by enhancing morphine-induced MOR endocytosis through the GRK2/β-arrestin2 pathway in vivo.

4. Discussion

In this study, we developed an mAb targeting MOR named 3A5C7 and tested the efficacy of mAb 3A5C7 in the treatment of morphine tolerance and dependence. We found that mAb 3A5C7 could facilitate MOR endocytosis in a GRK2/β-arrestin2-dependent manner and allow internalized MOR to recycle back to the cell surface. Moreover, mAb 3A5C7 attenuated morphine tolerance and dependence both in vitro and in vivo. Taken together, our study provides a novel therapeutic strategy to treat morphine tolerance using MOR-targeting mAbs.

Opioids have been well recognized for their effective analgesic effects and are widely prescribed in clinical practice. It was reported that approximately 90% of patients with chronic pain received opioids [9]. In spite of the universal utilization in pain treatment, chronic opioids are complicated with undesirable side effects, with tolerance among the most recognized ones [42]. Tolerance is defined as a gradual reduction in analgesic efficacy due to a decrease in opioid potency [43]. It would reduce the efficiency of the original dose of morphine to treat the same level of pain. The current management strategy for morphine tolerance is to increase the amount of drug [4]. However, tolerance is a developing and deteriorating process, so increasing the dose can only provide temporary relief rather than complete resolution. In our study, the mAb 3A5C7 coadministered with morphine chronically significantly alleviated the development of morphine tolerance in mice, suggesting that mAb 3A5C7 targeting MORs represents a novel option to treat morphine tolerance. Moreover, acute administration of mAb 3A5C7 at the time of morphine cessation also significantly attenuated withdrawal jumping caused by naloxone. Withdrawal jumping reflects the dependence on morphine, characterized by the development of aberrant physiological status after cessation of opioids, i.e., withdrawal syndrome including nausea, vomiting, diarrhea, insomnia, hypertension, tachycardia, mydriasis, and piloerection [34,36]. Collectively, the current results suggest that mAb 3A5C7, which targets MORs, is a competent candidate to treat morphine tolerance and dependence simultaneously and has the potential to be introduced into clinical practice in the future.

The analgesic effect of morphine occurs through the activation of MOR, causing the inhibition of AC and the resultant inhibition of high-threshold voltage-activated Ca^{2+} channels and the activation of inwardly rectifying K^{+} channels [44]. The mechanism of morphine tolerance is completely different. After being activated by opioids, MOR is phosphorylated at up to 20 potential phosphorylation sites in intracellular regions, contributing to receptor desensitization and endocytosis [20]. Although phosphorylation by both GRK and protein kinase C (PKC) promotes acute receptor desensitization, receptors phosphorylated by GRK often recruit β-arrestin and are then endocytosed and resensitized, while receptors phosphorylated by PKC, on the contrary, are resistant to endocytosis and/or resensitization [19]. MOR phosphorylated by GRKs, predominantly the GRK2 and GRK3 subtypes [20,45], recruits and interacts with β-arrestin2 at the plasma membrane [46], where β-arrestin2 promotes the uncoupling of MOR from the G protein and facilitates MOR endocytosis via a clathrin-dependent pathway [47]. Following endocytosis, MOR is dephosphorylated and recycled back to the plasma membrane in a reactivated state, which reinstates signal transduction [19,20]. Noticeably, morphine has a poor ability to induce endocytosis both in vitro [48] and in vivo [49]. Thus, desensitized MORs are poorly internalized and accumulate on the plasma membrane, resulting in morphine tolerance [50]. In our study, mAb 3A5C7 facilitated the endocytosis of MOR and thus alleviated morphine tolerance via the following mechanisms. First, coadministration of mAb 3A5C7 with morphine increased the expression level of GRK2, which subsequently facilitated the translocation of β-arrestin2 from the cytoplasm to the plasma membrane. Second, co-IP assays demonstrated that coadministration of mAb 3A5C7 with morphine increased the amount of GRK2 and β-arrestin2 recruited by MOR at the cell membrane. Moreover, we also determined that mAb 3A5C7 did not disturb the recycling of internalized MOR back to the plasma membrane, nor did it induce the internalized MOR to be loaded into lysosomes to be degraded. The facilitation of MOR endocytosis by mAb 3A5C7 by enhancing GRK2/β-arrestin2 signals was consistent with previous reports that overexpression of GRK2 and β-arrestin enhanced the induction of endocytosis by morphine [51,52]. Meanwhile, our study demonstrated that promoting MOR endocytosis alleviated morphine tolerance both in vivo and in vitro. This result is also in accordance with previous observations that the inclusion of extremely low-dose DAMGO, which was a strong endocytosis inducer and had no analgesic effects on its own at that dose, limited the development of morphine tolerance by stimulating the endocytosis of morphine-occupied MORs [53]. Similarly, another study reported a transgenic mouse in which part of the C-terminal region of the delta opioid receptor was substituted into MOR (rMOR). This rMOR was able to endocytose and recycle efficiently, and the mice with rMOR developed less morphine antinociceptive tolerance [54]. Taken together, our study not only demonstrated the efficacy of mAb 3A5C7 to treat morphine tolerance but also revealed that the molecular mechanisms of such effects of 3A5C7 were through facilitated MOR endocytosis via the GRK2/β-arrestin2 pathway.

In addition to the detrimental effects of tolerance and dependence caused by chronic morphine administration, exposure to low-dose morphine has been shown to protect against neuronal

damage caused by subsequent brain injuries, including ischemic stroke, neuroinflammation, and neurodegenerative diseases [55–57], a phenomenon known as preconditioning or hormesis. Hormesis is a biphasic dose response characterized by stimulation of low dose followed by inhibition at higher dose, with the maximum magnitude of the stimulatory effects being generally approximately 30%–60% greater than controls [58,59]. Preconditioning refers to protective effects against massive or even life-threatening toxic injuries by prior exposure to low doses of chemical or physical stressors [59]. It is now clear that hormesis could influence multiple neurobiological endpoints via direct stimulatory and/or preconditioning processes [59,60]. The protective effects of preconditioning and hormesis are mediated by molecular networks under the control of vitagenes, a group of genes encoding pro-survival proteins involved in preserving cellular homeostasis and redox balance during stressful conditions [58], such as heat shock protein, thioredoxin, sirtuin protein, and heme oxygenase-1 (HO-1) [61,62]. Notably, the expression of a battery of cytoprotective and antioxidant proteins is regulated by a common pathway, the Kelch-like epichlorohydrin-associated protein 1 (Keap1)/Nrf2/antioxidant response element (ARE) pathway [61]. Hormesis represents a universal and highly generalizable mechanism to increase resilience to environmental stress among species, and it can be evoked by different types of stimuli, such as exercise, dietary restriction, hypoxia, thermal extremes, radiation, and chemical or toxin exposure [59,63–65]. A case in point is nitric oxide (NO), a gaseous signaling molecule with a high dose being neurotoxic and a low dose being neuroprotective [66]. Some phytochemicals from natural plants can exert hormetic and neuroprotective effects by activating the Keap1/Nrf2/ARE pathway, including sulforaphane from cruciferous vegetable broccoli, curcumin from the East Indian herb *Curcuma longa* L., and hydroxytyrosol (HT) from olive in the Mediterranean diet, and HT has been made into an aqueous extract of olive pulp known as Hidrox® containing 40%–50% HT [61,67]. Similarly, hormesis and preconditioning apply well to morphine via numerous mechanisms. Repeated intake of high-dose morphine leads to antinociceptive tolerance, dependence, and addiction, accompanied by increased generation of reactive oxygen and nitrogen species [68], and decreased activities of antioxidant glutathione peroxidase and superoxide dismutase (SOD) [69]. In contrast, preconditioning with morphine exerts protective effects both peripherally and centrally. Peripherally, morphine preconditioning was reported to protect against subsequent myocardial ischemia via opioid receptors [70] and was associated with the inhibition of the mitochondrial permeability transition pore [71]. In the central nervous system, morphine preconditioning protected against neuronal damage from cerebral ischemia in an opioid receptor-dependent manner [57] and was mediated by balancing NO production [57], activating mammalian target of rapamycin and upregulating SOD [72], increasing catalase activity and the expression of anti-apoptotic B-cell lymphoma-2 (Bcl-2), and decreasing the levels of pro-apoptotic Bcl-2-associated X protein (Bax) [73]. Additionally, morphine preconditioning could exert anti-inflammatory effects in neuroinflammation models via opioid receptors [56,74]. Specifically, it was the δ1 opioid receptor, rather than MOR, κ opioid receptor, or δ2 opioid receptor, that mediated the protective effects of morphine preconditioning on microglial survival after lipopolysaccharide plus interferon-γ exposure [74]. Products of vitagene might contribute to morphine tolerance and preconditioning. Morphine tolerance was suggested to be regulated by the vitagene product sirtuin 1 [75]. It was also demonstrated that morphine exposure in primary human brain microvascular endothelial cells caused significant dysregulation of the Nrf2 pathway, leading to increased expression of HO-1, thioredoxin reductase 1, and peroxiredoxin-1 and jeopardized maximal mitochondrial respiration [76]. Taken together, neuroprotection of morphine preconditioning represents hormetic effects in morphine administration, bearing promising translational potential. However, it is tricky to balance between morphine preconditioning and the risks of dependence and tolerance. Whether mAb targeting opioid receptors could solve this dilemma, that is, to reinforce the protective effects of preconditioning and to avoid the development of tolerance and dependence, is worth exploring in future studies.

The successful development of the mAb 3A5C7 targeting MOR as a morphine tolerance inhibitor represents a major novelty of the current study. MOR belongs to the family of GPCRs with the typical structure of an extracellular N-terminus linked to seven α-helical transmembrane domains and an intracellular C-terminus [47]. GPCRs are membrane signal transmission receptor proteins encoded by nearly 4% of all human genomes [23] and are involved in many disorders such as cancer, infection, and cardiovascular diseases due to their functional diversities [25]. Thus, GPCRs are considered as the key molecular targets for drug discovery, accounting for over 30% of the targets of all currently marketed drugs [25]. Antibodies targeting GPCRs have emerged as superior therapeutics over traditional small-molecule drugs. Compared with small-molecule drugs, therapeutic antibodies possess higher target specificity, longer serum circulating half-life, and fewer side effects [24]. Nonetheless, although the first crystal structure of GPCRs was reported two decades ago [77], to date, there are only two approved anti-GPCR therapeutic antibody drugs, erenumab targeting calcitonin gene-related peptide receptor to treat migraine [78] and mogamulizumab targeting chemokine receptor 4 to treat refractory mycosis fungoides and Sézary syndrome [79]. Several reasons underlie the delay in the development of anti-GPCR antibodies, including high conformational variability and complexity, small exposed area of extracellular epitopes, difficulty in preparing active forms of GPCR antigen suitable for antibody isolation, and challenges in developing efficient antibody screening tools [24,25]. In the present study, we used a strategy of DNA immunization combined with cell immunization to prepare antibodies targeting MORs by hybridoma technology. We found that mAb 3A5C7 developed by this strategy had satisfactory specificity, affinity, and binding ability to MORs with spatial conformation. We did not carry out a surface plasmon resonance assay for affinity identification because we did not acquire the pure MOR antigen due to its seven-transmembrane structure. Moreover, the mAb 3A5C7 targeting MORs was able to modulate the endocytosis of MORs and thus alleviate morphine tolerance, confirming the functional activity and therapeutic potential of mAb 3A5C7. Taken together, the present procedure to successfully develop mAbs targeting MORs provides a methodological reference for preparing antibodies targeting GPCRs. The therapeutic efficacy of 3A5C7 mAb to inhibit morphine tolerance also provides a theoretical basis for future precision medicine to harness antibodies to treat MOR-related disorders such as pain and addiction [44].

In this study, mAb 3A5C7 enhanced the endocytosis of MORs induced by morphine. We also noticed that mAb 3A5C7 administered alone could not promote the internalization of MOR. This indicated that the mAb 3A5C7 exerted its therapeutic effects based on the facilitation of MOR internalization induced by morphine instead of directly inducing internalization. We surmised that this is because the mAb 3A5C7 induced a special conformation of the morphine-occupied MOR, which makes it easier to endocytose. Morphine binding and occupation induce spatial conformation changes in MOR, which are essential for signal transduction [47,80]. The recruitment and accessibility of GRKs and β-arrestin to MOR also require specific MOR spatial

conformation [44,50]. In the current study, we assume that the specific binding of mAb 3A5C7 to morphine-occupied MOR triggered a change in conformation of the morphine-occupied receptor, increasing its affinity and binding to GRK2 and recruitment of β-arrestin2, and finally promoting the endocytosis of morphine-bound MOR. The effect of mAb 3A5C7 is quite similar to that of an allosteric modulator of MOR, BMS-986122, which changed the conformation of MOR by rearranging the interactions between transmembrane helices 3 and 6 and increased the activity of MOR [81]. The exact binding sites of mAb to MOR as well as the mAb-induced conformational changes of MOR remain to be confirmed in further studies taking advantage of X-ray crystallography, cryo-electron microscopy, and nuclear magnetic resonance spectroscopy. In addition to attenuating morphine tolerance by enhancing morphine-induced MOR endocytosis, mAb 3A5C7 also exerted other biological functions. In our previous work, we found that MOR was highly expressed in cells and tissues of hepatocellular carcinoma (HCC) and was associated with the decreased survival of patients [26]. The 3A5C7 mAb could inhibit the proliferation of HCC cells by inhibiting the MOR-CD147-p53-mitogen-activated protein kinase (MAPK) pathway and enhance the cisplatin-induced apoptosis of HCC cells by downregulating phosphorylated extracellular signal-regulated kinase and Bcl-2 and upregulating Bax [26]. Thus, it can be deduced that the biological functions of 3A5C7 should be multifaceted, influencing various pathways linked to MOR. It also remains to be determined whether 3A5C7 exerts anti-tolerance effects via the MOR-CD147-p53-MAPK pathway. Future studies with high-throughput techniques such as RNA sequencing or proteome analysis would provide us with a more comprehensive profile of the biological functions of 3A5C7.

Several limitations should be noted in our study. First, we found that mAb-enhanced internalization occurred via the GRK2/β-arrestin2 pathway, while we did not investigate the mechanism underlying the recycling of MOR to the cell membrane, which remains to be elucidated in future studies. Second, the animal behavior experiments were based on the hotplate paradigm to test the thermal pain threshold under physiological conditions. Future studies are needed to verify the efficacy of mAb 3A5C7 in other pain paradigms and in pathological pain models. Third, our study focused on the tolerance and physical dependence associated with the analgesic effects of morphine. Future studies are needed to explore the effects of mAb 3A5C7 on psychological dependence or addiction.

5. Conclusions

In conclusion, in this study, we successfully developed a mAb 3A5C7 targeting MOR with high affinity, specificity, and binding ability to MOR antigen with spatial conformation. We found that the 3A5C7 mAb enhanced morphine-induced MOR endocytosis in a GRK2/β-arrestin2-dependent manner and attenuated morphine tolerance and dependence both in vitro and in vivo. The mAb 3A5C7 targeting MOR provides a new therapeutic strategy against morphine tolerance in the management of chronic pain, which bears promising translational value in future studies.

CRediT author statement

Jia-Jia Zhang: Methodology, Investigation, Formal analysis, Visualization, Writing - Original draft preparation; **Chang-Geng Song:** Methodology, Validation, Formal analysis, Visualization, Writing - Original draft preparation; **Miao Wang**, **Gai-Qin Zhang**, **Bin Wang**, **Xi Chen**, **Peng Lin**, and **Yu-Meng Zhu:** Investigation, Writing - Reviewing and Editing; **Zhi-Chuan Sun:** Methodology, Writing - Reviewing and Editing; **Ya-Zhou Wang**, **Jian-Li Jiang**, and **Ling Li:** Methodology, Resources, Writing - Reviewing and Editing; **Xiang-Min Yang:** Conceptualization, Methodology, Resources, Formal analysis, Funding acquisition, Writing - Reviewing and Editing; **Zhi-Nan Chen:** Conceptualization, Supervision, Resources, Funding acquisition, Formal analysis, Writing - Reviewing and Editing.

Declaration of competing interest

The authors declare that there are no conflicts of interest.

Acknowledgments

This work was supported by the National Basic Research Program of China (Grant No.: 2015CB553701) and the National Science and Technology Major Project, China (Grant No.: 2019ZX09732001).

Appendix A. Supplementary data

Supplementary data to this article can be found online at https://doi.org/10.1016/j.jpha.2023.06.008.

References

[1] H. Breivik, E. Eisenberg, T. O'Brien, The individual and societal burden of chronic pain in Europe: The case for strategic prioritisation and action to improve knowledge and availability of appropriate care, BMC Public Health 13 (2013), 1229.
[2] G. Corder, D.C. Castro, M.R. Bruchas, et al., Endogenous and exogenous opioids in pain, Annu. Rev. Neurosci. 41 (2018) 453–473.
[3] D.L. James, M. Jowza, Treating opioid dependence: Pain medicine physiology of tolerance and addiction, Clin. Obstet. Gynecol. 62 (2019) 87–97.
[4] S. Mercadante, E. Arcuri, A. Santoni, Opioid-induced tolerance and hyperalgesia, CNS Drugs 33 (2019) 943–955.
[5] O.P. Owodunni, M.H. Zaman, M. Ighani, et al., Opioid tolerance impacts compliance with enhanced recovery pathway after major abdominal surgery, Surgery 166 (2019) 1055–1060.
[6] P. Gulur, L. Williams, S. Chaudhary, et al., Opioid tolerance – a predictor of increased length of stay and higher readmission rates, Pain Physician 17 (2014) E503–E507.
[7] S. Mercadante, R.K. Portenoy, Opioid poorly-responsive cancer pain. Part 2: Basic mechanisms that could shift dose response for analgesia, J. Pain Symptom Manage. 21 (2001) 255–264.
[8] S. Sigismund, S. Confalonieri, A. Ciliberto, et al., Endocytosis and signaling: Cell logistics shape the eukaryotic cell plan, Physiol. Rev. 92 (2012) 273–366.
[9] P.P. Di Fiore, M. von Zastrow, Endocytosis, signaling, and beyond, Cold Spring Harb. Perspect. Biol. 6 (2014), a016865.
[10] G.J. Doherty, H.T. McMahon, Mechanisms of endocytosis, Annu. Rev. Biochem. 78 (2009) 857–902.
[11] C. Pathak, F.U. Vaidya, B.N. Waghela, et al., Insights of endocytosis signaling in health and disease, Int. J. Mol. Sci. 24 (2023), 2971.
[12] K. Sandvig, B. van Deurs, Endocytosis, intracellular transport, and cytotoxic action of Shiga toxin and ricin, Physiol. Rev. 76 (1996) 949–966.
[13] T. Spielmann, S. Gras, R. Sabitzki, et al., Endocytosis in *Plasmodium* and *Toxoplasma* parasites, Trends Parasitol. 36 (2020) 520–532.
[14] Y. Kojima, J.-P. Volkmer, K. McKenna, et al., CD47-blocking antibodies restore phagocytosis and prevent atherosclerosis, Nature 536 (2016) 86–90.
[15] I. Khan, P.S. Steeg, Endocytosis: A pivotal pathway for regulating metastasis, Br. J. Cancer 124 (2021) 66–75.
[16] C. Hall, H. Yu, E. Choi, Insulin receptor endocytosis in the pathophysiology of insulin resistance, Exp. Mol. Med. 52 (2020) 911–920.
[17] B.L. Heckmann, B.J.W. Teubner, B. Tummers, et al., LC3-associated endocytosis facilitates β-amyloid clearance and mitigates neurodegeneration in murine Alzheimer's disease, Cell 178 (2019) 536–551.e14.
[18] S. Wang, Historical review: Opiate addiction and opioid receptors, Cell Transplant. 28 (2019) 233–238.
[19] L. Martini, J.L. Whistler, The role of mu opioid receptor desensitization and endocytosis in morphine tolerance and dependence, Curr. Opin. Neurobiol. 17 (2007) 556–564.
[20] V.C. Dang, M.J. Christie, Mechanisms of rapid opioid receptor desensitization, resensitization and tolerance in brain neurons, Br. J. Pharmacol. 165 (2012) 1704–1716.
[21] T. Hashimoto, Y. Saito, K. Yamada, et al., Enhancement of morphine analgesic effect with induction of mu-opioid receptor endocytosis in rats, Anesthesiology 105 (2006) 574–580.

[22] X. Ma, R. Chen, M. Huang, et al., DAMGO-induced μ opioid receptor internalization and recycling restore morphine sensitivity in tolerant rat, Eur. J. Pharmacol. 878 (2020), 173118.
[23] C.J. Hutchings, A review of antibody-based therapeutics targeting G protein-coupled receptors: An update, Expert Opin. Biol. Ther. 20 (2020) 925–935.
[24] M.-S. Ju, S.T. Jung, Antigen design for successful isolation of highly challenging therapeutic anti-GPCR antibodies, Int. J. Mol. Sci. 21 (2020), 8240.
[25] M. Jo, S.T. Jung, Engineering therapeutic antibodies targeting G-protein-coupled receptors, Exp. Mol. Med. 48 (2016), e207.
[26] J.-J. Zhang, C.-G. Song, J.-M. Dai, et al., Inhibition of mu-opioid receptor suppresses proliferation of hepatocellular carcinoma cells via CD147-p53-MAPK cascade signaling pathway, Am. J. Transl. Res. 13 (2021) 3967–3986.
[27] F. Li, H. Ma, N. Wu, et al., IRAS modulates opioid tolerance and dependence by regulating μ opioid receptor trafficking, Mol. Neurobiol. 53 (2016) 4918–4930.
[28] P. Yang, X. Luo, J. Li, et al., Ionizing radiation upregulates glutamine metabolism and induces cell death via accumulation of reactive oxygen species, Oxid. Med. Cell. Longev. 2021 (2021), 5826932.
[29] S. Liu, Q. Wang, Z. Li, et al., TRPV1 Channel activated by the PGE2/EP4 pathway mediates spinal hypersensitivity in a mouse model of vertebral endplate degeneration, Oxid. Med. Cell. Longev. 2021 (2021), 9965737.
[30] M.K. Kaushik, K. Aritake, A. Imanishi, et al., Continuous intrathecal orexin delivery inhibits cataplexy in a murine model of narcolepsy, Proc. Natl. Acad. Sci. U S A 115 (2018) 6046–6051.
[31] C.R. Lin, M.H. Tai, J.T. Cheng, et al., Electroporation for direct spinal gene transfer in rats, Neurosci. Lett. 317 (2002) 1–4.
[32] M. Marsala, A.B. Malmberg, T.L. Yaksh, The spinal loop dialysis catheter: Characterization of use in the unanesthetized rat, J. Neurosci. Methods 62 (1995) 43–53.
[33] Y.-C. Chen, C.-F. Chiang, L.-F. Chen, et al., Polymersomes conjugated with des-octanoyl ghrelin for the delivery of therapeutic and imaging agents into brain tissues, Biomaterials 35 (2014) 2051–2065.
[34] J.-J. Zhang, C.-G. Song, J.-M. Dai, et al., Mechanism of opioid addiction and its intervention therapy: Focusing on the reward circuitry and mu-opioid receptor, MedComm (2020) 3 (2020), e148.
[35] T.F. Gamage, B.M. Ignatowska-Jankowska, P.P. Muldoon, et al., Differential effects of endocannabinoid catabolic inhibitors on morphine withdrawal in mice, Drug Alcohol Depend. 146 (2015) 7–16.
[36] B. Kest, C.A. Palmese, E. Hopkins, et al., Naloxone-precipitated withdrawal jumping in 11 inbred mouse strains: Evidence for common genetic mechanisms in acute and chronic morphine physical dependence, Neuroscience 115 (2002) 463–469.
[37] P.-K. Chao, H.-F. Chang, L.-C. Ou, et al., Convallatoxin enhance the ligand-induced mu-opioid receptor endocytosis and attenuate morphine antinociceptive tolerance in mice, Sci. Rep. 9 (2019), 2405.
[38] J. Ma, X. Yuan, H. Qu, et al., The role of reactive oxygen species in morphine addiction of SH-SY5Y cells, Life Sci. 124 (2015) 128–135.
[39] C.J. Hutchings, M. Koglin, W.C. Olson, et al., Opportunities for therapeutic antibodies directed at G-protein-coupled receptors, Nat. Rev. Drug Discov. 16 (2017), 661.
[40] P. Chan, K. Lutfy, Molecular changes in opioid addiction: The role of adenylyl cyclase and cAMP/PKA system, Prog. Mol. Biol. Transl. Sci. 137 (2016) 203–227.
[41] R. Binsack, M.-L. Zheng, Z.-S. Zhang, et al., Chronic morphine drinking establishes morphine tolerance, but not addiction in Wistar rats, J. Zhejiang Univ. Sci. B 7 (2006) 892–898.
[42] L.A. Colvin, F. Bull, T.G. Hales, Perioperative opioid analgesia-when is enough too much? A review of opioid-induced tolerance and hyperalgesia, Lancet 393 (2019) 1558–1568.
[43] R. Benyamin, A.M. Trescot, S. Datta, et al., Opioid complications and side effects, Pain Physician 11 (2008) S105–S120.
[44] J.T. Williams, S.L. Ingram, G. Henderson, et al., Regulation of μ-opioid receptors: Desensitization, phosphorylation, internalization, and tolerance, Pharmacol. Rev. 65 (2013) 223–254.
[45] A. Kovoor, J.P. Celver, A. Wu, et al., Agonist induced homologous desensitization of mu-opioid receptors mediated by G protein-coupled receptor kinases is dependent on agonist efficacy, Mol. Pharmacol. 54 (1998) 704–711.
[46] C.E. Groer, C.L. Schmid, A.M. Jaeger, et al., Agonist-directed interactions with specific beta-arrestins determine mu-opioid receptor trafficking, ubiquitination, and dephosphorylation, J. Biol. Chem. 286 (2011) 31731–31741.
[47] C. Stein, Opioid receptors, Annu. Rev. Med. 67 (2016) 433–451.
[48] D.E. Keith, S.R. Murray, P.A. Zaki, et al., Morphine activates opioid receptors without causing their rapid internalization, J. Biol. Chem. 271 (1996) 19021–19024.
[49] C. Sternini, M. Spann, B. Anton, et al., Agonist-selective endocytosis of mu opioid receptor by neurons *in vivo*, Proc. Natl. Acad. Sci. U S A 93 (1996) 9241–9246.
[50] T. Koch, V. Höllt, Role of receptor internalization in opioid tolerance and dependence, Pharmacol. Ther. 117 (2008) 199–206.
[51] J.L. Whistler, M. von Zastrow, Morphine-activated opioid receptors elude desensitization by beta-arrestin, Proc. Natl. Acad. Sci. U S A 95 (1998) 9914–9919.
[52] J. Zhang, S.S. Ferguson, L.S. Barak, et al., Role for G protein-coupled receptor kinase in agonist-specific regulation of mu-opioid receptor responsiveness, Proc. Natl. Acad. Sci. U S A 95 (1998) 7157–7162.
[53] L. He, J. Fong, M. von Zastrow, et al., Regulation of opioid receptor trafficking and morphine tolerance by receptor oligomerization, Cell 108 (2002) 271–282.
[54] J.A. Kim, S. Bartlett, L. He, et al., Morphine-induced receptor endocytosis in a novel knockin mouse reduces tolerance and dependence, Curr. Biol. 18 (2008) 129–135.
[55] B. Wang, C.-J. Su, T.-T. Liu, et al., The neuroprotection of low-dose morphine in cellular and animal models of Parkinson's disease through ameliorating endoplasmic reticulum (ER) stress and activating autophagy, Front. Mol. Neurosci. 11 (2018), 120.
[56] F. Rostami, S. Oryan, A. Ahmadiani, et al., Morphine preconditioning protects against LPS-induced neuroinflammation and memory deficit, J. Mol. Neurosci. 48 (2012) 22–34.
[57] M. Arabian, N. Aboutaleb, M. Soleimani, et al., Role of morphine preconditioning and nitric oxide following brain ischemia reperfusion injury in mice, Iran. J. Basic Med. Sci. 18 (2015) 14–21.
[58] V. Calabrese, C. Cornelius, A.T. Dinkova-Kostova, et al., Vitagenes, cellular stress response, and acetylcarnitine: Relevance to hormesis, Biofactors 35 (2009) 146–160.
[59] E.J. Calabrese, M.P. Mattson, G. Dhawan, et al., Hormesis: A potential strategic approach to the treatment of neurodegenerative disease, Int. Rev. Neurobiol. 155 (2020) 271–301.
[60] E.J. Calabrese, Preconditioning is hormesis part II: How the conditioning dose mediates protection: Dose optimization within temporal and mechanistic frameworks, Pharmacol. Res. 110 (2016) 265–275.
[61] V. Calabrese, C. Cornelius, A.T. Dinkova-Kostova, et al., Cellular stress responses, the hormesis paradigm, and vitagenes: Novel targets for therapeutic intervention in neurodegenerative disorders, Antioxid. Redox Signal. 13 (2010) 1763–1811.
[62] V. Calabrese, C. Cornelius, C. Mancuso, et al., Vitagenes, dietary antioxidants and neuroprotection in neurodegenerative diseases, Front. Biosci. (Landmark Ed.) 14 (2009) 376–397.
[63] D. Gems, L. Partridge, Stress-response hormesis and aging: "That which does not kill us makes us stronger", Cell Metab. 7 (2008) 200–203.
[64] E. Agathokleous, M. Kitao, E.J. Calabrese, Hormesis: Highly generalizable and beyond laboratory, Trends Plant Sci. 25 (2020) 1076–1086.
[65] E.J. Calabrese, Hormesis mediates acquired resilience: Using plant-derived chemicals to enhance health, Annu. Rev. Food Sci. Technol. 12 (2021) 355–381.
[66] V. Calabrese, C. Mancuso, M. Calvani, et al., Nitric oxide in the central nervous system: Neuroprotection versus neurotoxicity, Nat. Rev. Neurosci. 8 (2007) 766–775.
[67] R. Siracusa, M. Scuto, R. Fusco, et al., Anti-inflammatory and anti-oxidant activity of hidrox® in rotenone-induced Parkinson's disease in mice, Antioxidants (Basel) 9 (2020), 824.
[68] J. Skrabalova, Z. Drastichova, J. Novotny, Morphine as a potential oxidative stress-causing agent, Mini Rev. Org. Chem. 10 (2013) 367–372.
[69] A.O. Abdel-Zaher, M.G. Mostafa, H.S. Farghaly, et al., Role of oxidative stress and inducible nitric oxide synthase in morphine-induced tolerance and dependence in mice. Effect of alpha-lipoic acid, Behav. Brain Res. 247 (2013) 17–26.
[70] R. Li, G.T. Wong, T.M. Wong, et al., Intrathecal morphine preconditioning induces cardioprotection via activation of delta, kappa, and mu opioid receptors in rats, Anesth. Analg. 108 (2009) 23–29.
[71] M. Dorsch, F. Behmenburg, M. Raible, et al., Morphine-induced preconditioning: Involvement of protein kinase A and mitochondrial permeability transition pore, PLoS One 11 (2016), e0151025.
[72] M. Arabian, N. Aboutaleb, M. Soleimani, et al., Preconditioning with morphine protects hippocampal CA1 neurons from ischemia-reperfusion injury via activation of the mTOR pathway, Can. J. Physiol. Pharmacol. 96 (2018) 80–87.
[73] M. Arabian, N. Aboutaleb, M. Soleimani, et al., Activation of mitochondrial KATP channels mediates neuroprotection induced by chronic morphine preconditioning in hippocampal CA-1 neurons following cerebral ischemia, Adv. Med. Sci. 63 (2018) 213–219.
[74] M.-S. Gwak, L. Li, Z. Zuo, Morphine preconditioning reduces lipopolysaccharide and interferon-gamma-induced mouse microglial cell injury via delta 1 opioid receptor activation, Neuroscience 167 (2010) 256–260.
[75] X. He, P. Ou, K. Wu, et al., Resveratrol attenuates morphine antinociceptive tolerance via SIRT1 regulation in the rat spinal cord, Neurosci. Lett. 566 (2014) 55–60.
[76] S. Reymond, T. Vujić, D. Schvartz, et al., Morphine-induced modulation of Nrf2-antioxidant response element signaling pathway in primary human brain microvascular endothelial cells, Sci. Rep. 12 (2022), 4588.
[77] K. Palczewski, T. Kumasaka, T. Hori, et al., Crystal structure of rhodopsin: A G protein-coupled receptor, Science 289 (2000) 739–745.
[78] E. Dolgin, First GPCR-directed antibody passes approval milestone, Nat. Rev. Drug Discov. 17 (2018) 457–459.
[79] Y.L. Kasamon, H. Chen, R.A. de Claro, et al., FDA approval summary: Mogamulizumab-kpkc for mycosis fungoides and Sézary syndrome, Clin. Cancer Res. 25 (2019) 7275–7280.
[80] W. Huang, A. Manglik, A.J. Venkatakrishnan, et al., Structural insights into μ-opioid receptor activation, Nature 524 (2015) 315–321.
[81] S. Kaneko, S. Imai, N. Asao, et al., Activation mechanism of the μ-opioid receptor by an allosteric modulator, Proc. Natl. Acad. Sci. U S A 119 (2022), e2121918119.